Research Square

Preprints are preliminary reports that have not undergone peer review.
They should not be considered conclusive, used to inform clinical practice,
or referenced by the media as validated information.

HSD3B1 in prostate cancer prognosis and treatment

Jibira Yakubu
University Children's Hospital
Amit V. Pandey
amit.pandey@unibe.ch
University Children's Hospital

Systematic Review

Keywords: HSD3B1, rs1047303, prostate cancer, androgen deprivation, abiraterone, enzalutamide, predictive biomarker, pharmacogenetics

Posted Date: November 17th, 2026

DOI: https://doi.org/10.21203/rs.3.rs-11732724/v1

License: This work is licensed under a Creative Commons Attribution 4.0 International License.
Read Full License

Additional Declarations: No competing interests reported.

HSD3B1 in prostate cancer prognosis and treatment

Jibira Yakubu[1,2], Amit V. Pandey[1,2,3*]

[1]Pediatric Endocrinology, Diabetology and Metabolism, University Children's Hospital, Inselspital, 3010 Bern, Switzerland.

[2]Translational Hormone Research Program, Department of Biomedical Research, Faculty of Medicine, University of Bern, 3010 Bern, Switzerland.

[3]Department of Digital Medicine, University of Bern, 3008 Bern, Switzerland

*** For correspondence and reprint requests:**

Prof. Dr. Amit V Pandey
KIKL C837, Pediatric Endocrinology, University Children's Hospital Bern,
Freiburgstrasse 15, 3010 Bern Switzerland
Tel: 0041 31 632 9637 Email: amit.pandey@unibe.ch
ORCID: https://orcid.org/0000-0001-8331-5902

Running title: HSD3B1 genotype and prostate cancer therapy

Keywords: HSD3B1; rs1047303; prostate cancer; androgen deprivation; abiraterone; enzalutamide; predictive biomarker; pharmacogenetics.

Disclosure Statement: The authors have nothing to disclose.

Abstract

Inherited variation in *HSD3B1*, which encodes 3β-hydroxysteroid dehydrogenase type 1, alters the stability of a key enzyme in peripheral steroid metabolism and offers a compelling mechanism for continued androgen production during prostate cancer treatment. The adrenal-permissive rs1047303 allele has been associated with poorer outcomes after androgen deprivation, particularly in some patients with low-volume metastatic disease. Yet its clinical significance is not uniform across disease stages, ancestral populations or modern treatment regimens. Biomarker analyses from randomized trials show that treatment intensification with enzalutamide provides benefit across *HSD3B1* genotypes, without convincing evidence that the variant modifies relative treatment efficacy. Studies of castration-resistant disease are further complicated by differences in prior treatment, genetic models and clinical risk adjustment. HSD3B1 also participates in abiraterone metabolism, creating opposing pharmacological effects that complicate simple predictions. Here we critically evaluate the mechanistic, clinical and population evidence, distinguish prognostic associations from treatment-predictive biomarkers, and define the evidence needed for prospective clinical implementation. HSD3B1 remains a promising marker of steroid metabolic biology, but current evidence does not justify genotype-guided selection or withholding of established systemic therapies.

Keywords: HSD3B1; rs1047303; prostate cancer; androgen deprivation; abiraterone; enzalutamide; predictive biomarker; pharmacogenetics.

Key points

1. Inherited *HSD3B1* rs1047303 alters 3βHSD1 protein stability, influencing peripheral androgen production and offering a mechanistic basis for altered prostate cancer progression.
2. Adrenal-permissive *HSD3B1* genotypes are associated with adverse prognosis in some androgen deprivation cohorts, particularly low-volume metastatic disease, but findings depend on clinical context.
3. Randomized biomarker analyses have not established a reproducible *HSD3B1*-by-treatment interaction that warrants selection or withholding of enzalutamide, docetaxel or other standard therapies.
4. 3βHSD1 participates in both androgen biosynthesis and abiraterone metabolism, generating biologically opposing metabolites and complicating straightforward pharmacogenetic predictions.
5. Ancestry-associated allele frequencies, genotype contrast models, cohort selection and clinical risk adjustment materially influence reported outcomes and the transferability of findings.

6. Clinical implementation requires prespecified randomized interaction analyses, ancestry-aware validation, absolute benefit–harm assessment and evidence of improved decisions beyond established risk markers.

Glossary

Adrenal-permissive allele. The HSD3B1 rs1047303 C allele associated with greater 3βHSD1 protein persistence and increased capacity to use adrenal-derived steroid precursors.

Adrenal-restrictive genotype. The HSD3B1 AA genotype in the conventional clinical literature, associated with less persistent 3βHSD1 protein.

Intracrine androgen synthesis. Production of biologically active androgens within a tissue from locally available or circulating precursors.

Prognostic biomarker. A marker associated with clinical outcome irrespective of whether it changes the relative effect of a particular treatment.

Predictive biomarker. A marker that identifies a difference in treatment effect between therapeutic alternatives, ideally supported by an adequately powered interaction analysis.

Genotype-by-treatment interaction. A statistical test of whether the relative effect of a treatment differs according to genotype.

Metastatic hormone-sensitive prostate cancer. Metastatic prostate cancer that remains responsive to androgen suppression.

Castration-resistant prostate cancer. Prostate cancer that progresses despite castrate concentrations of circulating testosterone.

Dominant genetic model. A comparison combining heterozygous and homozygous C-allele carriers (AC/CC) against AA.

Recessive genetic model. A comparison of CC homozygotes against AA and AC combined.

Introduction

Human 3β-hydroxysteroid dehydrogenase/Δ5–Δ4 isomerase type 1 (HSD3B1) is an NAD^+-dependent enzyme that converts pregnenolone to progesterone and dehydroepiandrosterone to androstenedione, serving as a critical upstream component of peripheral androgen and estrogen synthesis [1]. Expressed predominantly in the placenta and peripheral tissues, *HSD3B1* is distinct from the HSD3B2 isoenzyme, which is primarily expressed in the adrenal and gonad tissues. Inherited coding and regulatory variants in HSD3B1 significantly govern cellular enzyme abundance and expression patterns [2]. The common missense variant rs1047303, historically designated 1245A>C, alters the amino acid sequence, distinguishing a relatively unstable wild-type protein (367N) from a highly persistent, degradative-resistant form (367T) that facilitates sustained peripheral steroidogenesis. Beyond its documented role in prostate cancer, homozygous inheritance of the permissive allele is implicated in other hormone-driven phenotypes. It correlates with an elevated risk of estrogen receptor-positive postmenopausal breast cancer, as well as higher rates of distant metastasis and breast cancer-specific mortality in independent postmenopausal breast cancer validation cohorts [3,4]. In contrast, the adrenal-restrictive genotype is overrepresented in relatively hormone-independent endometrial and breast cancer subtypes [5]. These associations also extend to non-malignant conditions; for instance, the restrictive genotype is associated with poorer lung function among patients with severe asthma receiving daily oral glucocorticoids [6]. These broad systemic effects demonstrate that *HSD3B1* acts as a context-dependent modifier of systemic steroid availability and disease phenotypes rather than operating as a universally deleterious allele or an established treatment-selection marker.

The mechanistic relevance of *HSD3B1* in prostate cancer depends on this differential enzyme stability. Chang and colleagues established that the 367T form resists ubiquitin-mediated degradation, thereby driving intracrine androgen synthesis in preclinical models of castration-resistant prostate cancer [7]. This mechanism represents a gain in effective steroidogenic capacity achieved through protein persistence, rather than alteration in intrinsic catalytic turnover. While these structural findings render inherited HSD3B1 variations unusually interpretable from a biological standpoint, they do not inherently determine which systemic treatment a patient should receive.

Biochemically, the primary reaction that utilizes adrenal precursor is the conversion of DHEA to androstenedione, a process that combines 3β-hydroxysteroid oxidation with Δ5-to-Δ4 isomerization. Downstream enzymes subsequently convert androstenedione into testosterone and dihydrotestosterone (DHT) [1,8]. Thus, 3βHSD1 facilitates a multi-step enzymatic route to potent androgens but it does not directly convert DHEA to dihydrotestosterone in a single step. The clinical designation "adrenal-permissive" characterizes the tumor's capacity to utilize adrenal-derived steroid precursors; it does not

imply that *HSD3B1* expression is restricted to or localized within the adrenal glands themselves (**Figure 1**) [8].

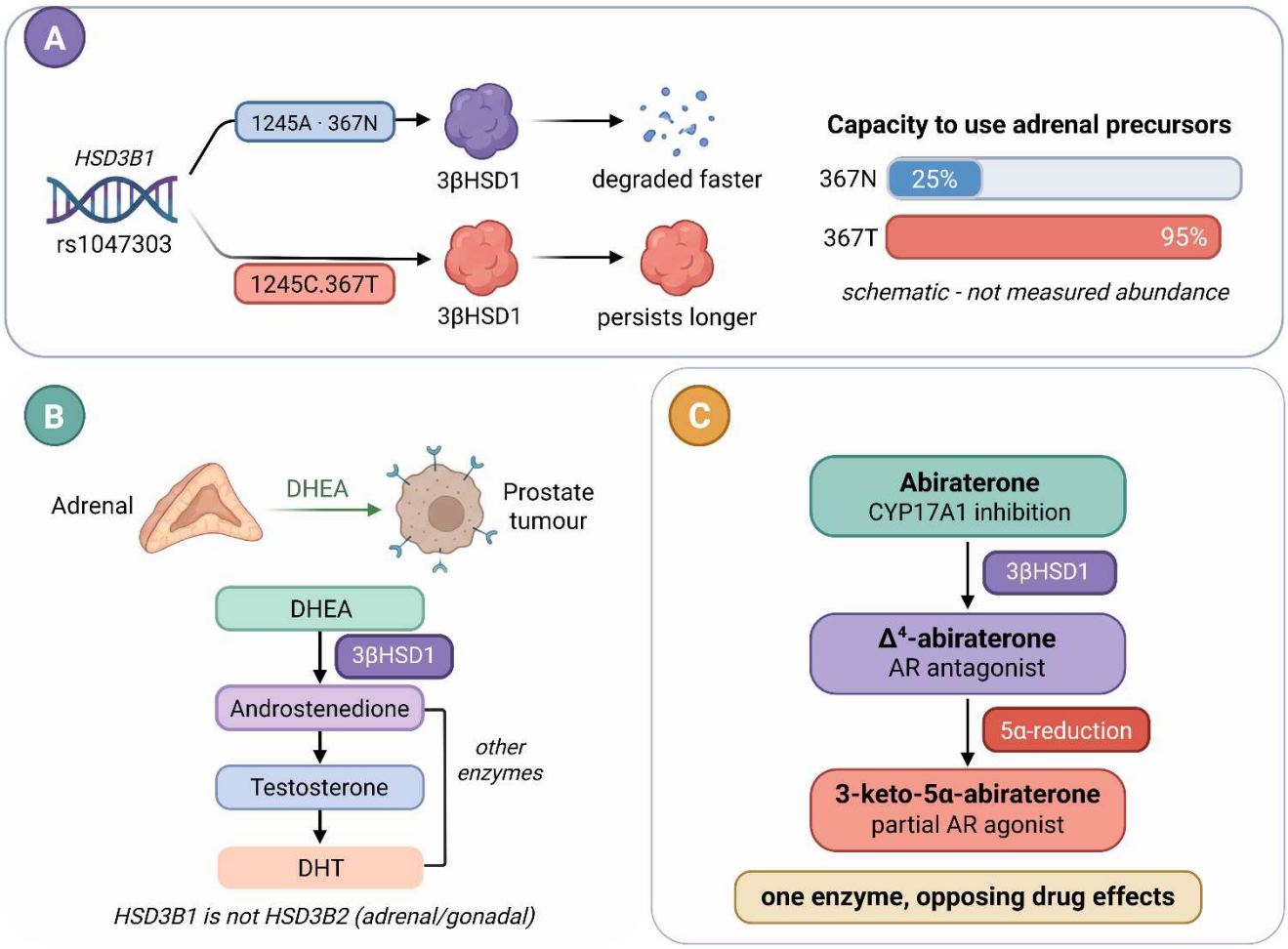


Figure 1. HSD3B1 links inherited variation to steroid and drug metabolism. A, HSD3B1 rs1047303 is shown using the historical 1245A/C notation alongside the protein designations. The permissive 367T protein resists degradation more than the 367N protein, increasing enzyme persistence and the capacity to use adrenal precursors [7]. **B**, adrenal-derived DHEA supplies a precursor for steroid metabolism in prostate tumor cells. 3βHSD1 converts DHEA to androstenedione; other enzymes convert androstenedione to testosterone and dihydrotestosterone (DHT). DHEA can be converted into DHT through a series of enzymes present in prostate cancer cells. Peripheral HSD3B1 is distinct from HSD3B2 which is the predominant adrenal and gonadal isoenzyme. **C**, abiraterone inhibits CYP17A1 and is metabolized by 3βHSD1 to Δ4-abiraterone that can act as an androgen receptor (AR) antagonist; subsequent 5α-reduction produces 3-keto-5α-abiraterone, which has partial AR agonist activity [9]. Recent mechanistic work further illustrates the complexity of 3βHSD1-mediated steroid metabolism during therapy [10].

A clinical report by Hearn and colleagues linked the historically designated *HSD3B1* 1245C allele to inferior clinical outcomes following androgen deprivation across three independent patient cohorts totaling 443 individuals [11]. Although early publications frequently labeled these associations as

"predictive," a biomarker that correlates with outcomes during a single treatment modality is fundamentally prognostic of underlying disease biology, not necessarily predictive of a differential clinical benefit between two distinct interventions. This review strictly reserves the term "predictive" for clinical evidence derived from comparative analyses that assess whether a treatment's therapeutic effect differs significantly by patient genotype.

Consequently, translating HSD3B1 into clinical practice requires answering three distinct questions:

1. Does the genotype identify a distinct baseline risk of disease progression or death?
2. Does the genotype modify the relative therapeutic effect of a specific treatment compared with a contemporary alternative?
3. Does integrating genotypic data improve clinical decision-making enough to alter final patient outcomes?

A definitive answer to the first question cannot substitute for the second or third. HSD3B1 may be a biologically causal and prognostically informative marker in specific clinical settings, but it still lacks the treatment-discriminating capacity required for routine patient selection. Answering these clinical questions requires a defined framework that combines database mining, statistical pooling, and co-occurrence modeling. Defined workflows allow us to query thousands of patient records across primary and metastatic datasets to track how HSD3B1 and HSD3B2 alter as the prostate cancer progresses. Computational meta-analysis then isolates specific patient sub-cohorts, pools survival estimates across independent trials, and maps how these metabolic alterations co-occur with major tumor driver genes. By combining large-scale genomic data mining with clinical outcomes, we can evaluate both the baseline prognostic risk of these variants and their true utility as predictive tools for treatment selection.

Search and critical review methods

Here we performed a critical translational review utilizing an auditable, targeted search strategy; it is not a registered systematic review or an individual-participant-data meta-analysis. PubMed was queried using the search string HSD3B1 AND prostate, restricted to articles published up to 8 October 2026, which yielded 113 unique records. A supplementary search incorporating rs1047303, the full enzyme name, and the title of the first mutation paper identified five additional records for screening. Publisher databases, PubMed Central, clinical trial registries, and international conference proceedings were searched to identify updated data for the ARCHES, ENZAMET, and STAMPEDE trials, as well as recent ancestry-specific datasets.

All citations were verified against PubMed XML or publisher metadata. Full-text articles were retrieved when available, and peer-reviewed abstracts were used when complete texts or online

supplements were unavailable. The eligible evidence baseline included original human genotype–outcome studies, biomarker correlational analyses of randomized controlled trials, pharmacodynamic investigations, and mechanistic laboratory studies that are vital for clinical interpretation. Review articles were utilized for background verification, but were excluded from independent cohort counts. Studies were classified by publication status: peer-reviewed full articles, conference abstracts, or preprints. Early abstracts were not treated as independent observations if the final, fully peer-reviewed manuscript had already been published. To avoid artificial inflation of data, cohorts demonstrating overlapping enrollment periods, identical institutional participation, or matched sample sizes were audited for potential duplication rather than assumed to be independent.

For each clinical dataset, the appraisal evaluated the specific disease setting at treatment initiation, metastatic volume, disease timing (de novo versus recurrent), country or reported genetic ancestry, treatment combinations, prior exposure to novel antiandrogens or taxanes, the biospecimen type utilized, the genetic contrast model, clinical endpoints, time origins, and covariate adjustments. Patient nationality or geographic treatment site was not equated with genetically inferred ancestry. Treatment randomization was strictly distinguished from genotype distribution. While biomarker studies embedded within randomized trials provide robust estimates, they remain vulnerable to selection bias if only an incomplete subset of the randomized population provides scorable DNA. Adjusted hazard ratios (aHRs) were selected as the primary metric for prognostic synthesis, and unadjusted estimates are explicitly labeled as such. Clinical endpoints, including overall survival (OS), prostate cancer-specific mortality (PCSM), radiographic progression-free survival (rPFS), clinical progression, PSA progression, treatment failure, and time to castration resistance, were treated as separate entities and were not used interchangeably. Cause-specific and sub-distribution hazard ratios were analyzed separately. Reported genetic contrasts were retained exactly as published: dominant (AC/CC vs. AA), recessive (CC vs. AA/AC), categorical (AC vs. AA and CC vs. AA), or additive (per-C-allele) models.

Primary quantitative pooling required independent cohorts with compatible disease states, treatment backbones, endpoints, time origins, genetic models, and statistical adjustments (**Table 1**). Because contemporary treatment-interaction estimates did not meet these standardization criteria, a formal primary meta-analysis could not be justified. An exploratory, restricted summary was conducted solely to evaluate the prognostic association between the permissive genotype and OS in low-volume metastatic disease using data from the CHAARTED trial and the conference-level STAMPEDE analysis. This exploration excludes ENZAMET due to differences in antiandrogen exposure and highly selective cohort criteria. Log hazard ratios were weighted by inverse variance, with standard errors reconstructed from published 95% confidence intervals (CIs). Inter-study heterogeneity was evaluated using Cochran's Q and the I^2 statistic. Random-effects modeling and a modified Hartung-Knapp interval adjustment were applied as conservative sensitivity checks to evaluate statistical stability.

Computational Methods and Genomic Data Integration

Data Acquisition and API Query Controls

Somatic mutation counts, copy-number alteration (CNA) profiles, and multi-locus co-occurrence matrices were queried from the cBioPortal for Cancer Genomics RESTful interface [12,13]. To benchmark primary prostate adenocarcinoma tissue, the pipeline isolated the National Cancer Institute's GDC PanCancer Atlas cohort (prad_tcga_pan_can_atlas_2018, n=492 profiles) [14]. To model advanced adaptive biology under treatment-driven selection pressure, metastatic castration-resistant lines were extracted using the Stand Up To Cancer/Prostate Cancer Foundation Dream Team dataset (prad_su2c_2019, n=444 profiles) [15]. Targeted genomic coordinates isolated the human 3β-hydroxysteroid dehydrogenase isoenzyme loci using fixed Entrez identifiers 3283 (HSD3B1) and 3284 (HSD3B2). Baseline germline stratification frequencies for the missense single-nucleotide polymorphism (SNP) rs1047303 (c.1100A>C, p.Asn367Thr) were compiled from the Genome Aggregation Database (gnomAD v4.0) across genetically inferred continental ancestral blocks to control for population stratification.

Meta-analytic pooling and subclonal co-occurrence mapping

A quantitative fixed-effects meta-analysis pooling data on overall survival in low-volume metastatic hormone-sensitive prostate cancer (mHSPC) was performed using inverse-variance weighting of log-transformed hazard ratios (**Figure 9**). Reconstructed standard errors were modeled natively using absolute confidence intervals extracted from the primary peer-reviewed CHAARTED cohort 37.2% weight) and the STAMPEDE trial platform abstract 62.8% weight). Cross-trial heterogeneity was assessed using Cochran's Q statistic and the I^2 statistic. To evaluate the structural relationship between advanced metabolic selection and classical tumor suppressors, Boolean overlap algorithms mapped the concurrent distribution of HSD3B1 amplifications against PTEN homozygous deletions, TP53 mutations, and RB1 loss sequences within the metastatic cohort (**Figure 7**).

Software and Graphics Pipeline

All software code and genomic cleaning matrices were compiled using a native Python 3.13 pipeline. Data structure handling was controlled via Pandas (v2.2) and NumPy (v1.26). Geometric layouts, log-axis transformations for error bars, horizontal multi-locus tracks, and discrete oncoprint tile grids were rendered using Matplotlib (v3.9), with patient columns sorted in descending order of metabolic complexity to isolate subclonal dependencies.

Results

Genotype definitions and biological hypotheses

To ensure consistency, the initial 1245A>C notation and the official rs1047303 identifier should be reported together. Under current reference sequence nomenclature, the variant is officially designated NM_000862.3: c.1100A>C, p.(Asn367Thr). The initial 1245A>C terminology stems from an older transcript definition that was widely used in early literature. Historical transcript positions should not be used in place of modern HGVS coding notation. Furthermore, while clinical literature frequently cites the N367T substitution, current reference sequence orientations may describe the reciprocal substitution depending on the defined genomic strand. Consequently, clinical assay reports must explicitly state the transcript accession number and version, the reference allele, the specific strand, and the predicted protein consequence. The A and C allele designations are retained in this review to maintain consistency with the published clinical literature.

The choice of genetic model dictates statistical findings. A dominant model (AC/CC vs. AA) tests whether the presence of any permissive allele alters clinical outcomes. A recessive model (CC vs. AA/AC) evaluates whether two copies of the permissive allele are required to drive the phenotype. A categorical model independently calculates estimates for AC versus AA and CC versus AA. In contrast, an additive model presumes a constant, linear change in log hazard per copy of the C allele. These models represent distinct statistical questions rather than interchangeable terminologies. Some clinical papers have grouped heterozygous AC patients into an "adrenal-restrictive" category in recessive analyses, despite the biochemical persistence of the single-variant allele. Reporting explicit genotype counts is preferable to relying solely on these descriptive phenotypic labels.

Moreover, genetic model selection can become confounded by patient ancestry. Applying a recessive model within a population where the CC genotype is rare yields low statistical power and unstable event counts. Conversely, a dominant model may be mathematically estimable within the same cohort but cannot address the underlying biological question of recessivity. Selecting a genetic model post hoc based on the lowest derived P-value artificially inflates the strength of evidence. Clinical protocols should prespecify a primary genetic contrast model, report all absolute genotype counts and event rates, and relegate secondary models to formal sensitivity sections.

Table 1: Clinical evidence by disease setting. HRs are genotype associations unless explicitly labeled as treatment effects. The study location is not a genetic ancestry assignment. Abbreviations: ADT, androgen deprivation therapy; ARPI, androgen receptor pathway inhibitor; BCR, biochemical recurrence; CRPC, castration-resistant prostate cancer; mHSPC, metastatic hormone-sensitive prostate cancer; OS, overall survival; PCSM, prostate cancer-specific mortality; PFS, progression-free survival. Confidence intervals are 95%.

Study	Setting and population	Exposure and contrast	Finding and limitations
Hearn JWD 2016 [11]	Recurrent/metastatic US; 443 in 3 cohorts	ADT; categorical and dominant	Adjusted primary dominant PFS 1.6 (1.0–2.7) Retrospective; metastatic cohort selected after CRPC
Agarwal N 2017 [16]	mHSPC US; 102	ADT; CC vs AA	Adjusted PFS 2.16 (1.01–4.58) Small CC group; not a treatment interaction
Wu G 2015 [17]	Advanced HSPC China; 103	Surgical castration; AC vs AA	Higher CRPC proportion; no time-to-event difference Do not equate event proportion with hazard.
Hearn JWD 2018 [18]	BCR after radiotherapy US; 213	ADT; CC vs AA	Adjusted metastasis 2.01 (1.02–3.97) Not a definitive radiotherapy treatment prediction
Shiota M 2019 [19]	HSPC / CRPC Japan; 104 / 99	ADT or abiraterone; dominant	Abiraterone adjusted OS 0.48 (0.16–1.25) Separate settings; 0 CC in abiraterone cohort
Shiota M 2022 [20]	Advanced HSPC Japan; 194	ADT; AC/CC vs AA	Adverse adjusted PFS in low volume Numerical adjusted HR not verified; possible overlap.
Shi R 2026 [21]	HSPC and subsequent CRPC China; 785	ADT and later ARPIs; dominant/additive	ADT-only n=438: adjusted CRPC HR 2.37 (1.49–3.77) Later, differences in drug subgroups do not prove interaction.
Hearn JWD 2020 [22]	mHSPC White participants: 475	ADT ± docetaxel; dominant	Low-volume adjusted OS 1.74 (1.01–3.00) No established docetaxel interaction
Sharifi N 2024a [23] **(ARCHES)**	mHSPC Multinational; 660	Enzalutamide + ADT vs placebo + ADT; dominant	OS treatment interaction P=0.44 Subset genotyped; crossover; low-volume events are sparse.
Sharifi N 2024b [24] **(ENZAMET)**	Low-volume mHSPC ENZAMET; 287	ADT + AR antagonist; dominant	Pooled-arm genotype OS 0.55 (0.36–0.84), unadjusted No ADT-only arm; no concurrent docetaxel
Hahn AW 2018 [25]	mCRPC US; 76	First-line abiraterone + prednisone	No independent PFS association Numerical adjusted estimate not verified.

Lu C 2020 [26]	mCRPC UK/US; 266	First-line abiraterone/enzalutamide; recessive	Adjusted OS 1.78 (1.03–3.07) 22 CC; no randomized alternative comparison
Khalaf DJ 2020 [27]	mCRPC Canada/Spain; 547	Abiraterone/enzalutamide; recessive	Adjusted progression association not significant Do not pool unadjusted HR as adjusted.
Stangl-Kremser J 2019 [28]	CRPC Tumor-based; 44	Mixed second-line systemic therapy	No survival association established Tumor genotype is not necessarily germline.
Vaz-Ferreira A 2024 [29]	mCRPC after localized diagnosis Portugal; subgroup 24 of 123	Abiraterone; dominant	Adjusted OS 3.28 (1.07–9.95) Selected small subgroup; multiple comparisons
Almassi N 2018 [30]	mCRPC US; 90	Ketoconazole; allele dosage	Longer duration/progression intervals with C Historical nonrandomized; not abiraterone
Shiota M 2023 [31]	CRPC Japan; multiple treatments	Docetaxel vs ARPIs; multilocus models	Differential SNP associations explored Nonrandomized; multiplicity; numeric interaction not extracted.
Shiota M 2021 [32]	CRPC Japan; 99	Abiraterone; HSD3B1 + SRD5A2	Combined-genotype treatment-failure association Potential overlap with 2019 cohort
Shiota M 2023 [33]	CRPC Japan; 21	Abiraterone + dutasteride	Metabolite modulation; PSA responses Single-arm; not survival validation
McKay RR 2024 [34]	Across stages US veterans: 5,287	Heterogeneous; recessive/categorical	Higher PCSM with CC Prognosis, not drug selection
Lu L 2026 [35]	Incident PC UK Biobank; 14,644	Population cohort; competing risks	No HSD3B1 association with cumulative PCSM Do not pool with cause-specific hazards.

Historical androgen deprivation therapy and recurrent disease

The foundational multicohort study by Hearn and colleagues provided strong clinical evidence supporting the intracrine steroidogenesis hypothesis, but its hazard estimates should not be viewed as a universal baseline effect [11]. In their primary post-prostatectomy cohort, the adjusted dominant-model progression estimate was 1.6 (95% CI, 1.0–2.7; P=0.074), with more pronounced hazard ratios observed among homozygous CC carriers and for advanced endpoints [11]. However, because their metastatic validation cohort was assembled retrospectively from men who had already developed castration resistance, the reconstruction of early ADT outcomes remains vulnerable to selection and survival biases. These early data support subsequent replication rather than unrestricted transportability to modern first-line treatment combinations.

An independent validation series involving 102 men with newly diagnosed metastatic hormone-sensitive prostate cancer (mHSPC) reported an inferior progression-free survival for the CC versus AA genotype following multivariable adjustment for Gleason score and baseline PSA (HR 2.16; 95% CI 1.01-4.58) [16]. However, this wide confidence interval highlights a statistical instability, and because the contrast evaluated CC versus AA specifically, it cannot be pooled directly with dominant-model datasets.

In a Chinese cohort of 103 patients undergoing surgical castration, carriers of the AC genotype had a higher raw proportion of castration resistance over time, but the study did not show a significant reduction in time to castration resistance or an increase in disease-specific mortality [17]. This distinction emphasizes that an absolute event proportion over a fixed follow-up must not be conflated with a time-to-event hazard rate. This early cohort serves as an important scientific counterweight to the assumption that all historical datasets yielded uniform survival reductions.

Among the 213 men receiving salvage ADT for biochemical recurrence following definitive radiotherapy, the adjusted hazard ratio for developing metastasis was significantly higher in CC versus AA patients (aHR 2.01; 95% CI 1.02-3.97) [18]. In contrast, progression-free and overall survival endpoints were not clearly separated by genotype in this cohort. Variable exposures to first-generation antiandrogens and subsequent lines of therapy make comparisons between post-radiotherapy and post-prostatectomy salvage populations difficult to interpret. Crucially, metastatic progression during salvage ADT should not be utilized as a proxy for evaluating a patient's primary response to definitive radiotherapy itself.

Early Japanese primary ADT data included 104 patients, but only nine individuals carried the AC or CC genotypes; within this limited cohort, the reported progression association paradoxically favored the wild-type AA genotype[19]. A subsequent Japanese multi-institutional analysis of 194 patients noted an adverse, adjusted prognostic association restricted to low-volume disease, while no separation was observed in high-volume settings [20]. Given the related institutional context of these two reports, a rigorous overlap audit is mandatory before any pooling attempts, as clinical consistency across separate papers does not guarantee statistical independence of the underlying patients.

A larger 2026 Chinese observational study evaluated 785 patients and reported an adjusted dominant-model hazard ratio for time to castration resistance of 1.62 (95% CI, 1.10-2.40). Within the subset of 438 patients managed with ADT alone, the hazard ratio rose to 2.37 (95% CI 1.49-3.77) [21].

While these data confirm an ADT-resistance phenotype within an East Asian clinical setting, the cohort differed substantially from Western studies in its baseline treatment compositions and covariate models. Because statistical adjustments in this study were restricted principally to disease stage and grade, the potential for residual confounding remains high. Furthermore, additive and dominant hazard ratios extracted from the same patient population must not be treated as independent data points.

Metastatic hormone-sensitive prostate cancer

CHAARTED

The biomarker analysis of the phase III CHAARTED trial evaluated 475 self-reported White men, comparing the AC/CC genotypes against the wild-type AA baseline. In patients with low-volume metastatic disease, the adjusted hazard ratios for carriers were 1.89 for time to castration resistance (95% CI 1.13-3.14) and 1.74 for overall mortality (95% CI 1.01-3.00) [22]. No corresponding prognostic separations were observed within the high-volume metastatic strata. Most importantly, the formal statistical analysis demonstrated no significant genotype-by-docetaxel interaction. Therefore, an inferior prognosis among permissive-allele carriers cannot be used to justify clinically selecting for or withholding docetaxel based on HSD3B1 status. Additionally, restricting genomic analysis to White participants limits the direct generalizability of these findings to broader populations with different allele frequencies and distinct post-progression treatment patterns (**Figure 2**).

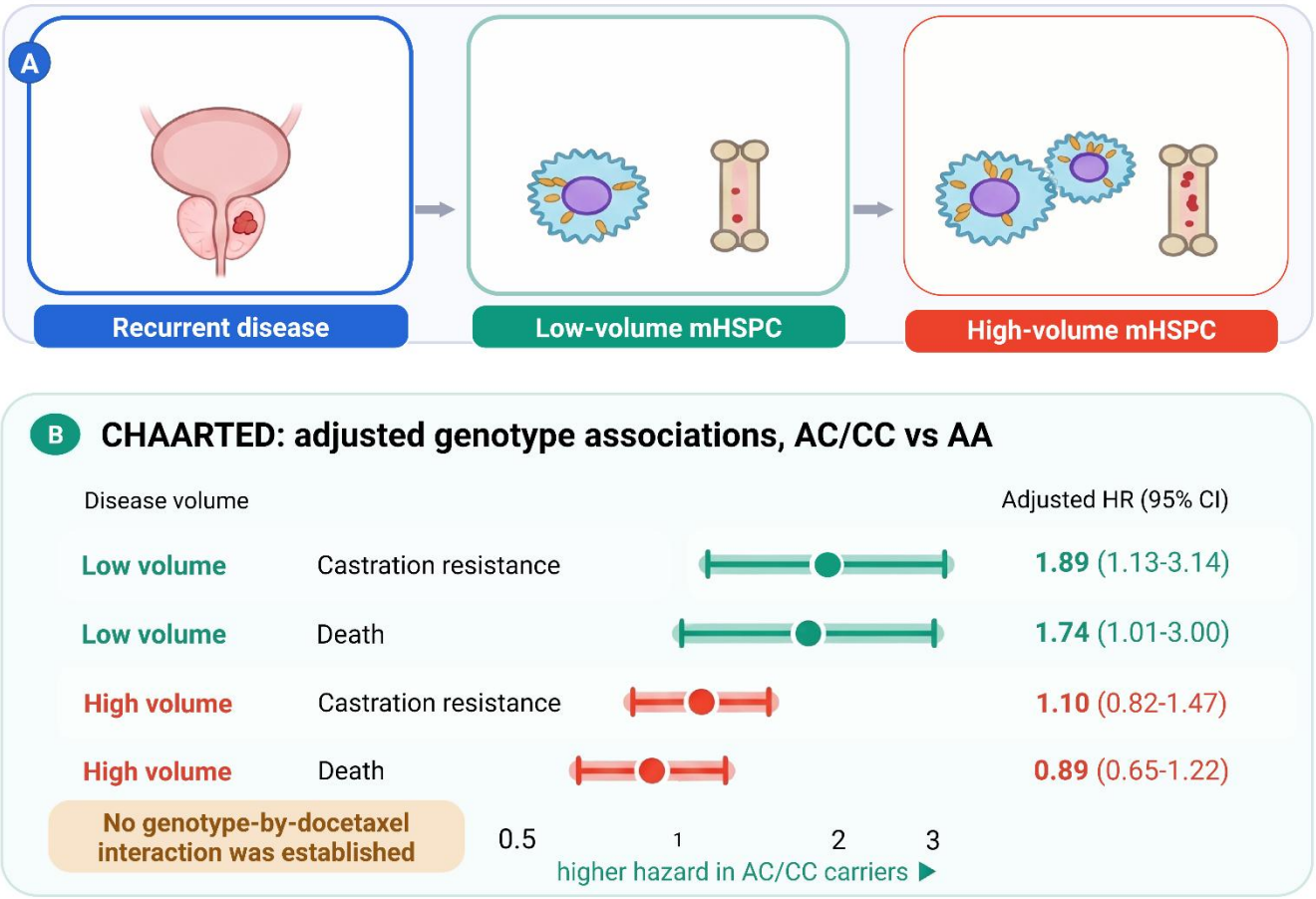


Figure 2: **Genotype prognosis depends on disease and treatment context. A**, Illustrative recurrent, low-volume metastatic hormone-sensitive prostate cancer (mHSPC) and high-volume mHSPC settings. **B**, Adjusted CHAARTED hazard ratios (HRs) compare AC/CC with AA for castration resistance and death, stratified by disease volume. The adjusted low-volume HRs are 1.89 (95% CI: 1.13-3.14) for time to castration resistance and 1.74 (95% CI: 1.01–3.00) for overall survival; corresponding high-volume HRs are 1.10 (95% CI: 0.82-1.47) and 0.89 (95% CI: 0.65-1.22), respectively.

ARCHES

The phase III ARCHES trial successfully genotyped 660 randomized participants evaluating the addition of enzalutamide to ADT versus placebo plus ADT [23]. The treatment hazard ratios for rPFS favored the addition of enzalutamide in both the AA cohort (HR 0.66; 95% CI 0.48–0.92) and the AC/CC cohort (HR 0.62; 95% CI 0.44-0.88). Similarly, treatment hazard ratios for OS favored enzalutamide intensification in both groups (AA: HR 0.55, 95% CI 0.37-0.83; AC/CC: HR 0.67, 95% CI 0.46-0.98). The formal interaction P-values were highly non-significant at 0.76 for rPFS and 0.44 for OS. When analyzing the pure prognostic impact of genotype across both arms, the stratified genotype-associated survival comparison was 1.29 (95% CI, 0.99-1.70), indicating an adverse signal but not excluding the null hypothesis. These data strongly support the clinical efficacy of enzalutamide across all HSD3B1 genotypes rather than providing a rationale for withholding intensified therapy. Specific limitations bind interpretation of these data: only a subset of the total randomized trial population provided scorable DNA,

low-volume survival events were sparse at the time of analysis, and open-label treatment crossover complicates mature survival assessments. The trial cohort also included a subset of patients who had previously received docetaxel chemotherapy. In reporting these results, direct randomized treatment contrasts within genotypic strata must be presented separately from non-randomized genotype-associated prognostic contrasts (**Figure 3**).

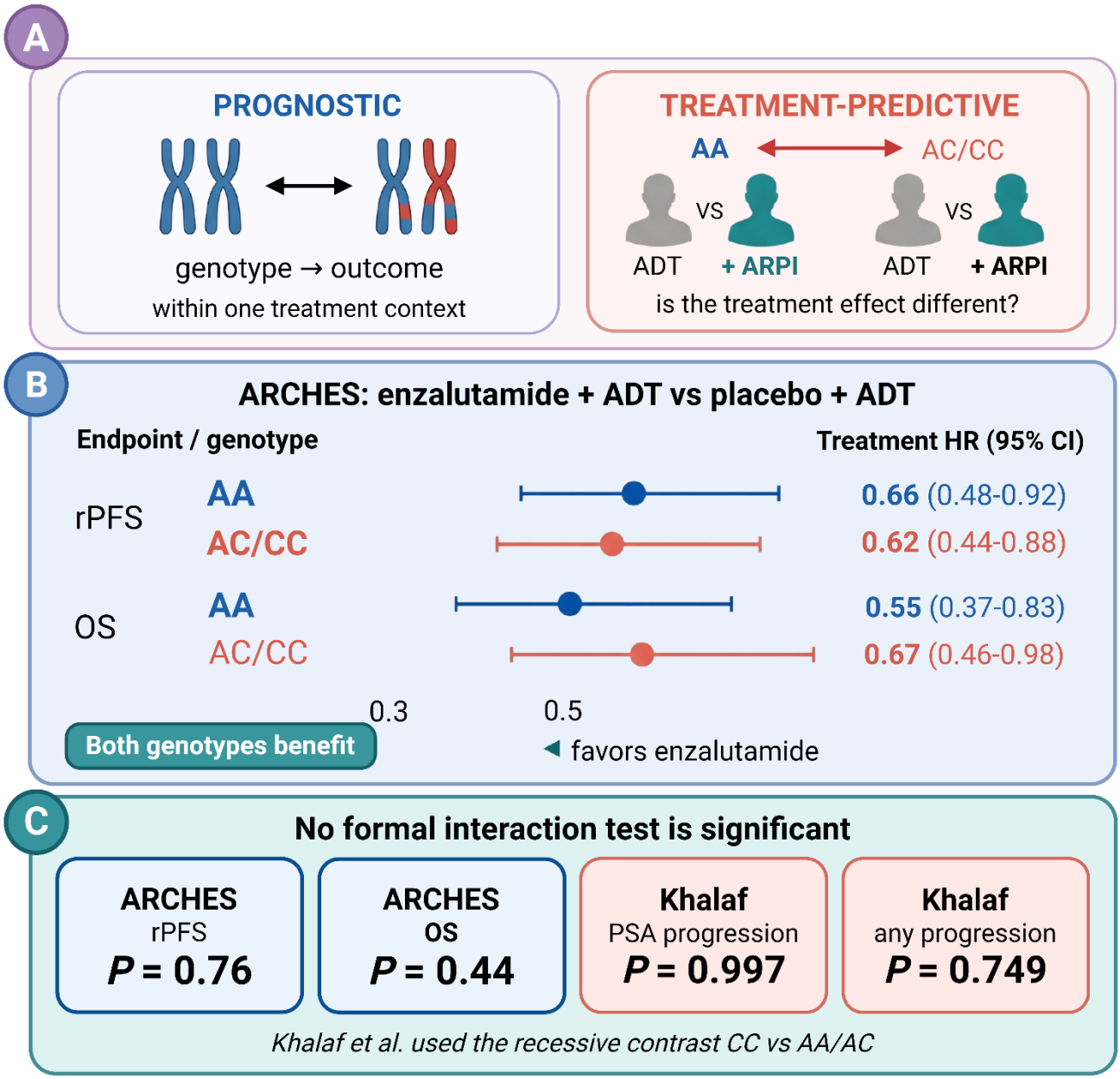


Figure 3: **Differentiating prognostic association and treatment interaction. A**, A prognostic analysis compares genotype-associated outcomes within a treatment context, whereas a treatment-predictive analysis compares randomized treatment effects across genotypes. **B**, ARCHES stratified treatment HRs compare enzalutamide plus androgen deprivation therapy (ADT) with placebo plus ADT within AA and AC/CC groups for radiographic progression-free survival (rPFS) and overall survival (OS). **C**, Formal interaction P-values are shown for ARCHES rPFS (P = 0.76) and OS (P = 0.44), establishing that the clinical survival benefit of enzalutamide intensification is preserved regardless of a patient's HSD3B1 status [23,27].

ENZAMET

A correlational analysis from the phase III ENZAMET trial specifically included 287 men with low-volume metastatic disease who received ADT plus either enzalutamide or a first-generation nonsteroidal antiandrogen, and explicitly excluded patients who received concurrent docetaxel [24]. Within this highly selected cohort, AC/CC carriers paradoxically demonstrated superior pooled-arm overall survival compared to AA wild-type patients (HR 0.55; 95% CI 0.36-0.84). This favorable prognostic association remained statistically significant in multivariable models. However, this quoted hazard ratio represents a pooled-arm genotype comparison; it is not an adjusted estimate of randomized treatment interaction. Because both treatment arms in this analysis actively blocked the androgen receptor, and because these patients had extensive access to subsequent lines of life-prolonging therapies, these data support a complex hypothesis of context-dependent androgen dependence. The study cannot demonstrate a reversal of the adverse prognostic signal relative to standard ADT alone because a pure ADT control arm was not included in this selected stratum. Ultimately, both genotype groups derived substantial clinical benefit from early intensification with enzalutamide.

The apparent discrepancies between these large phase III trials are highly instructive for clinical trial design. CHAARTED, ARCHES, and ENZAMET differed fundamentally in their comparator backbones, baseline chemotherapy exposures, biomarker selection criteria, metastatic volume distributions, event maturities, and post-progression therapies. Cross-trial comparisons cannot isolate which of these clinical variables explains the changing prognostic genotype associations. A genetic marker may correlate with baseline clinical risk and absolute treatment benefit without demonstrating a significant multiplicative hazard ratio interaction on a forest plot. Taking this into account, the absence of a statistically significant interaction test is not definitive proof of therapeutic equivalence and the statistical precision and the range of clinically compatible interaction effects must be considered.

Characterization of Other Combinations

The published evidence does not establish a clinical role for HSD3B1 testing in guiding contemporary triplet therapy (ADT plus docetaxel plus an ARPI). Furthermore, these data do not support the use of genotype to preferentially select among advanced agents such as abiraterone, enzalutamide, apalutamide, or darolutamide in hormone-sensitive disease. Prior docetaxel exposure within the ARCHES trial represents a different clinical scenario than a randomized, concurrent triplet intervention. Similarly, the selected ENZAMET cohort explicitly omitted concurrent docetaxel and cannot resolve this clinical question. Biomarker outcomes derived from regimens combining enzalutamide and abiraterone simultaneously cannot isolate the independent therapeutic contribution of either drug.

Castration-resistant prostate cancer

Abiraterone metabolism and cross-reactivity

In addition to inhibiting CYP17A1 to block DHEA production, abiraterone also inhibits other steroid metabolizing enzymes, including CYP21A2 thereby affecting cortisol production [36]. The impact of HSD3B1 on patient outcomes during abiraterone therapy is bi-directional because the enzyme modulates both endogenous intra-tumoral steroids and exogenous drug metabolism. Alyamani and colleagues showed that inheritance of the permissive allele significantly accelerates the metabolic conversion of abiraterone to 3-keto-5α-abiraterone, a metabolite that acts as a partial structural agonist of the androgen receptor [9]. This metabolic cascade requires an initial 3βHSD1-dependent oxidation to Δ4-abiraterone, followed by downstream 5α-reduction by separate enzymes. Consequently, enhanced enzymatic flux through 3βHSD1 leads to competing biochemical outcomes, producing both potent androgen receptor antagonists and active agonists within the tumor microenvironment. A superior capacity to utilize adrenal precursors does not automatically translate into a greater net clinical benefit from abiraterone, and these distinct pharmacodynamic metabolite variations have not been validated as surrogates for overall survival.

A 2026 mechanistic study further illustrated this enzymatic complexity, demonstrating that 3βHSD1 facilitates the reverse regeneration of DHT from 3β-androstanediol and the regeneration of an active abiraterone metabolite [10]. While the correlative component of this work (utilizing the PANTHER cohort) evaluated abiraterone, apalutamide, and prednisone, it extends the known biological mechanism beyond the simple DHEA metabolism. It does not, however, provide definitive evidence of a genotype-by-treatment interaction in survival, nor does it establish the clinical superiority of that specific drug combination.

Clinical studies of abiraterone and enzalutamide

Hahn and colleagues evaluated 76 men initiating first-line abiraterone acetate plus prednisone for mCRPC and reported no statistically independent association between HSD3B1 genotype and progression-free survival. While the small sample size limits the ability to rule out modest variations in hazard, this null finding must be integrated into the literature to avoid selective reporting bias [25]. In a Japanese mCRPC cohort comprising 99 patients managed with abiraterone, 14 individuals carried the heterozygous AC genotype, and none carried the homozygous CC genotype [19]. The study reported an adjusted treatment-failure hazard ratio of 0.35 (95% CI 0.13-0.80) favoring AC carriers. However, the frequently cited favorable overall survival hazard ratio of 0.40 was entirely unadjusted; following formal

multivariable adjustment, the OS hazard ratio attenuated to 0.48 (95% CI 0.16-1.25), crossing the statistical null. Interpretation of these data is further complicated by the heavily pretreated baseline characteristics of the cohort: nearly half had received prior enzalutamide, and a substantial proportion had progressed on prior docetaxel. This represents a mixed-line, AC-versus-AA evaluation that cannot be directly compared with Western clinical datasets that use a homozygous recessive model.

Lu and colleagues evaluated first-line abiraterone or enzalutamide therapy in a cohort of 266 patients with metastatic castration-resistant prostate cancer (mCRPC), capturing 22 individuals who carried the homozygous variant CC genotype. The adjusted hazard ratio for overall survival comparing CC with the combined AA/AC cohort was 1.78 (95% CI: 1.03–3.07), indicating a significantly worse prognostic baseline that was not overridden by modern AR receptor axis-targeted therapies [26]. Interestingly, objective PSA response rates and absolute treatment durations did not differ significantly between the genetic cohorts. While this study provides evidence of an adverse prognostic association under these contemporary therapies, it cannot prove that CC carriers derive less relative benefit from these drugs than they would from an alternative intervention, such as early chemotherapy. Furthermore, while statistical models adjusted for age, Gleason score, baseline PSA, prior chemotherapy, and baseline metastatic status, they cannot fully eliminate residual confounding stemming from clinical selection or subsequent treatment sequencing.

Khalaf and colleagues conducted a robust analysis of 547 patients pooled from two prospective trials, one an open-label randomized trial comparing initial abiraterone versus enzalutamide, and the other an investigator-selected observational cohort [27]. The raw, unadjusted progression hazard ratio for the recessive contrast (CC vs. AA/AC) was directionally adverse at 1.31 (95% CI 1.02-1.67). However, this association lost independent statistical significance following multivariable adjustment. Formal treatment-interaction tests comparing abiraterone against enzalutamide efficacy were strictly negative for both PSA progression (P=0.997) and any clinical/radiographic progression (P=0.749) (Figure 3). Methodologically, unadjusted estimates must not be pooled with adjusted models, and a non-significant adjusted analysis must be reported precisely rather than assigned an arbitrary hazard ratio of 1.0.

A small tumor-tissue-based series evaluating 44 advanced prostate cancer patients (with 39 contributing to the second-line analysis) failed to establish a statistically significant survival association [28]. Using tumor tissue presents distinct genetic challenges compared with standardized germline testing from whole blood. Somatic copy number acquisitions, allelic imbalances, variable tumor purity, and therapy-driven clonal selection can alter the observed tissue genotype. Consequently, tumor-only tissue sequencing datasets should not be automatically pooled with confirmed germline registries.

Vaz-Ferreira and colleagues reported a hospital-based cohort of 123 patients with mCRPC [29]. A statistically significant genotype association emerged only in a highly restricted subgroup of 24 abiraterone-treated patients with strict nonmetastatic disease at the time of initial diagnosis, yielding an adjusted OS hazard ratio of 3.28 (95% CI, 1.07-9.95) for AC/CC versus AA. Crucially, the full, unselected

cohort failed to demonstrate this survival separation. Post hoc model selection, multiple subgroup adjustments, and wide confidence intervals render these specific data hypothesis-generating rather than an independent validation of a universal biomarker (**Figure 4**).

In the 2026 Chinese dataset, abiraterone clinical response correlated with C-allele status, whereas enzalutamide response did not, with reported within-arm hazard ratios of 3.22 and 0.98, respectively [21]. However, demonstrating a significant within-arm association in one cohort, alongside a non-significant association in another, does not, by itself, establish a differential treatment effect between the two drugs. A formal, cross-arm statistical interaction test, a direct confidence interval for the interaction coefficient, strict controls for treatment selection bias, and standardized clinical response criteria are mandatory before these data can be interpreted as a therapeutic selection rule.

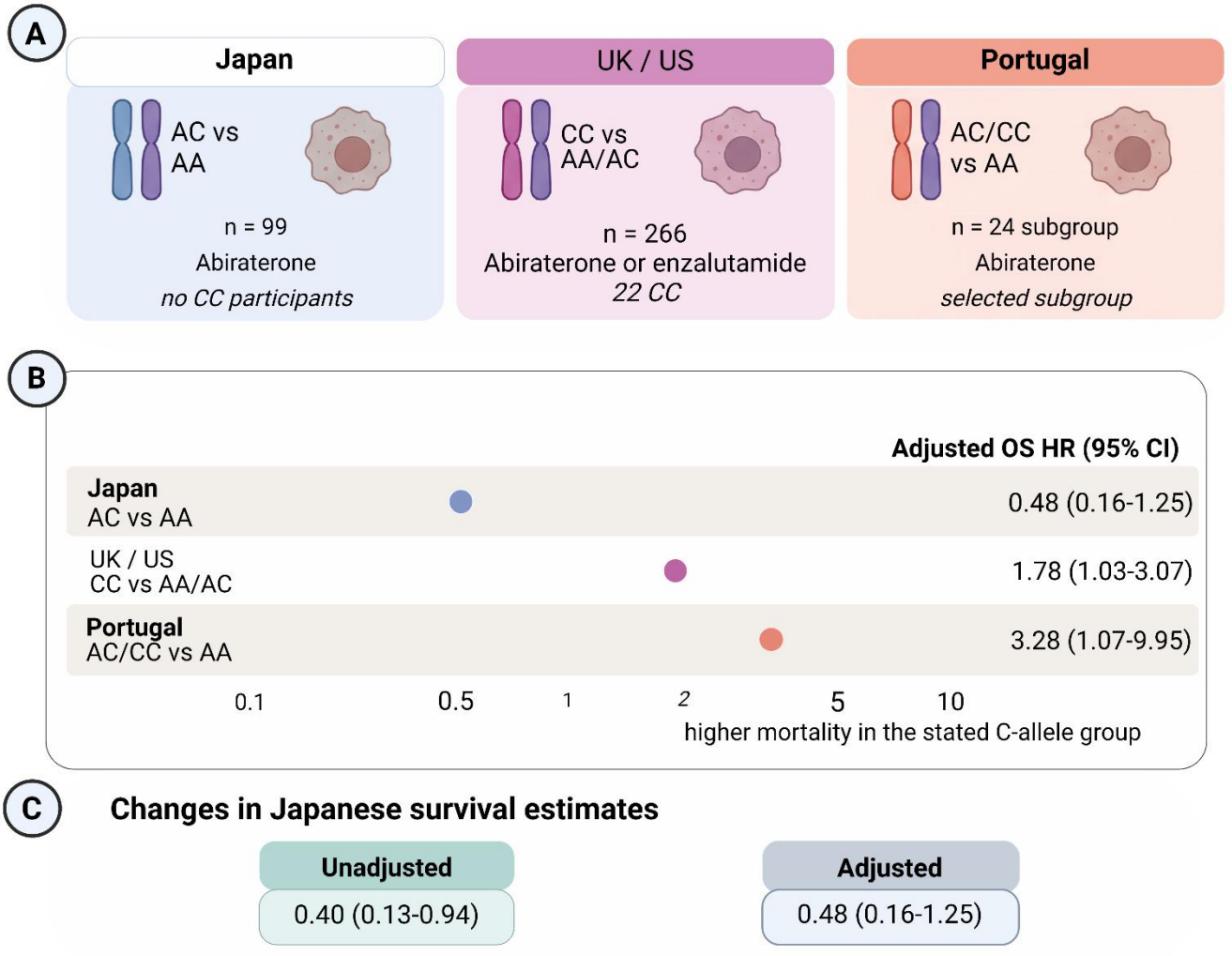


Figure 4: Genetic analysis in Castration resistant cohorts. A, three cohorts contributing contrasting genotype-associated OS estimates: the Japanese abiraterone cohort (n=99; AC versus AA, with no CC participants)[19], the UK/US first-line abiraterone or enzalutamide cohort (n=266; CC versus AA/AC) [26], and the selected Portuguese abiraterone subgroup initially diagnosed without metastases (n=24; AC/CC versus AA) [29]. Country labels identify study recruitment and do not establish genetically inferred ancestry. **B**, adjusted OS HRs and 95% CIs on a logarithmic axis. HR >1 indicates higher mortality in the stated C-allele group. **C**, the Japanese unadjusted OS estimate of 0.40 (0.13–0.94) becomes 0.48 (0.16–1.25)

after adjustment [19]. Differences in prior therapy, genotype model, and clinical selection preclude a common pooled interpretation: the Japanese cohort included substantial prior exposure to enzalutamide and docetaxel, whereas the Portuguese result came from a small, selected subgroup.

Other interventions and multilocus genetic models

Almassi and colleagues evaluated 90 patients managed with the nonsteroidal CYP17A1 inhibitor ketoconazole, observing a linear prolongation of treatment duration and progression-free intervals that matched increasing numbers of the permissive C allele [30]. While these findings offer valuable historical context regarding the suppression of non-gonadal steroid pathways, ketoconazole is pharmacologically distinct from steroidal agents such as abiraterone and was not compared with a randomized alternative. These observational data should not be pooled with contemporary ARPI datasets to infer a broad, class-wide therapeutic interaction.

Shiota and colleagues investigated complex, multi-variant pharmacogenetic models to explore differential single-nucleotide polymorphism (SNP) associations between docetaxel chemotherapy and novel ARPIs [31]. While multi-variant interaction testing is conceptually relevant to therapeutic discrimination, these non-randomized treatment allocations remain highly vulnerable to statistical overfitting and require extensive external validation. They do not support a clinically validated HSD3B1-only treatment-selection algorithm.

A separate multi-locus analysis combining HSD3B1 and SRD5A2 genotypes in 99 Japanese abiraterone-treated patients reported improved prognostic separation compared to single-gene models [32]. However, given that this study used the same sample size and institutional timeline as their prior single-gene report, these data should be treated as potentially overlapping rather than as independent validation. Furthermore, a combined multi-locus hazard ratio cannot be interpreted as a pure HSD3B1 effect. A subsequent single-arm phase II trial evaluating a combination of abiraterone and the 5α-reductase inhibitor dutasteride in 21 patients demonstrated notable modulation of serum metabolites and encouraging objective PSA responses, but lacked a randomized control group [33]. Neither multi-locus associations nor clear pharmacodynamic target engagement proves that adding dutasteride prolongs overall survival within a specific genotypic stratum.

Prognosis across populations and ancestry

A large-scale analysis from the Million Veteran Program (MVP) evaluated 5,287 patients across various stages of disease, capturing 91 prostate cancer deaths specifically among patients tracking advanced endpoints [34]. The homozygous CC genotype correlated with an elevated risk of prostate cancer-specific mortality, demonstrating a 5-year cumulative incidence of 4.0% for CC compared to 2.1% for AC and 1.9% for the wild-type AA cohort. While these robust data support a recessive prognostic hypothesis,

they cannot isolate a specific contemporary drug interaction. Furthermore, clinical models restricted exclusively to patients who subsequently develop metastatic disease are heavily conditioned on post-diagnosis clinical events and require highly cautious interpretation.

In contrast, a 2026 population-based incident cohort from the UK Biobank tracking 14,644 prostate cancer patients reported no statistically significant association between HSD3B1 genotype and cumulative prostate cancer-specific mortality in rigorous competing-risk analyses [35]. Discrepancies between these large datasets are likely driven by variations in patient ascertainment criteria, baseline clinical risk structures, genotype coding styles, variable systemic treatment exposures, and distinct statistical models. Methodologically, a Fine-Gray sub-distribution hazard ratio and a cause-specific Cox hazard ratio are not numerically interchangeable, and neither model directly answers whether an ARPI should be selected or withheld based on genotype.

Patient ancestry introduces critical variables regarding allele prevalence, statistical precision, linkage disequilibrium blocks, and the specific clinical settings in which a genotype is discovered. Ancestry also correlates strongly with access to systemic healthcare, medical comorbidities, clinical stage at initial presentation, and subsequent treatment sequences. In the ARCHES biomarker cohort, only 8 genotyped individuals were reported as Black or African American, of whom 1 was an AC/CC carrier. This sparse distribution is statistically insufficient to draw ancestry-specific treatment-interaction conclusions. Geographic replication across international boundaries is scientifically valuable, but it does not eliminate the confounding effects of population stratification; an isolated Japanese or Chinese cohort must not be treated as a uniform representative for all Asian populations globally (**Figure 5**) [23].

Cohorts assembled retrospectively after disease progression are inherently enriched for specific genotypes, treatment survivors, or distinct molecular tumor subtypes. This selection pressure can generate prognostic associations that are completely absent within an unselected incident population. While an individual's germline genotype is biologically fixed at birth, their selection into an advanced, treated clinical cohort is highly dynamic. Future genetic analyses must transparently report calculated genetic ancestry principal components rather than relying solely on self-identified race. Studies should clearly display genotype-specific absolute event counts and true absolute risks within defined clinical strata. The primary goal of translational oncologic research must be transportable biological inference rather than race-based prescribing algorithms.

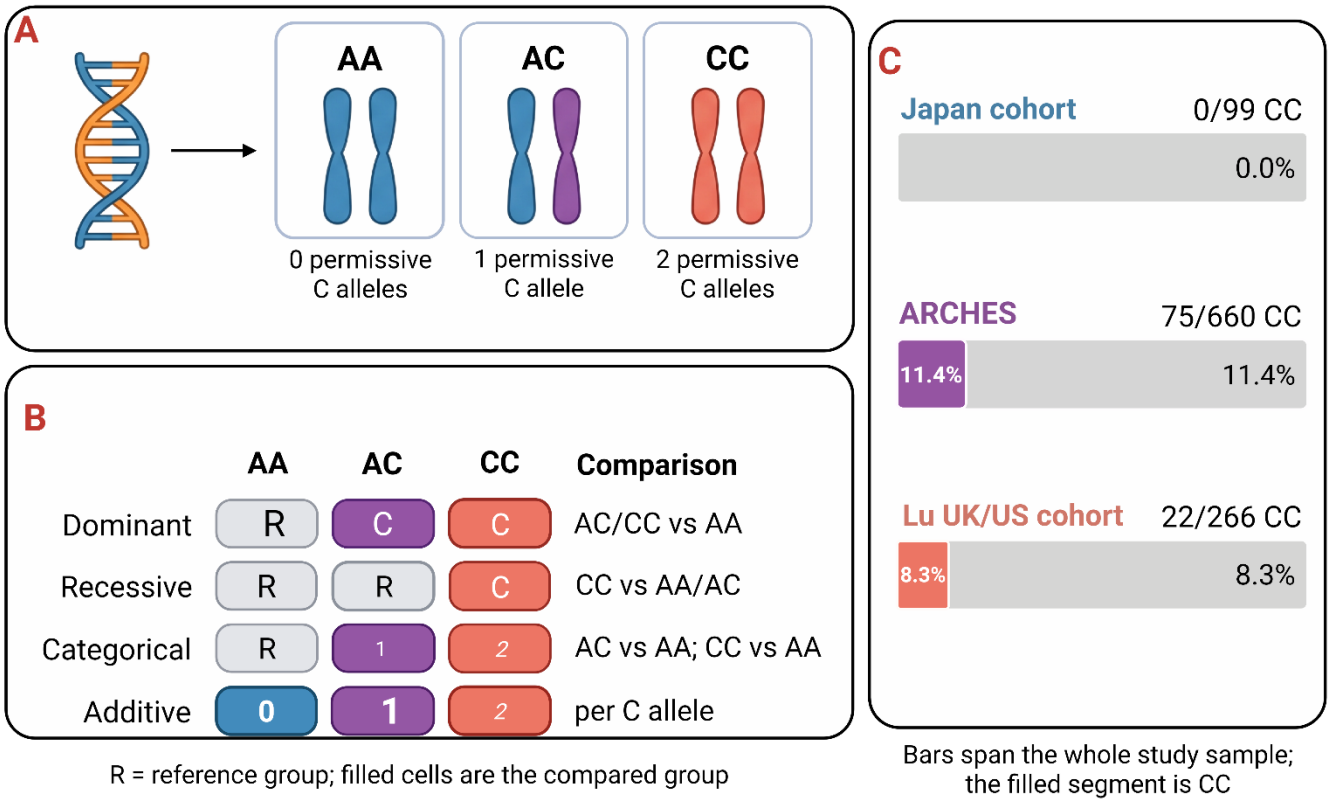


Figure 5: Evidence by Genotype model and representation. A, AA, AC, and CC correspond to zero, one, and two copies of the historically designated permissive C allele. **B**, dominant, recessive, categorical, and additive models define different contrasts. R denotes the reference group, and C denotes membership of the carrier comparison group in the first two rows. In the categorical row, 1 and 2 identify separate AC and CC effects relative to AA; they do not affect sizes. In the additive row, 0, 1, and 2 are allele counts under a constant per-allele log-hazard assumption. **C**, CC representation in selected study samples: 0/99 in the Japanese abiraterone cohort [19], 75/660 in ARCHES [23], and 22/266 in the Lu UK/US cohort [26]. Each bar represents the entire study sample: the darker segment represents CC, and the lighter remainder represents AA/AC. Proportions are drawn from exact counts and labeled to one decimal place.

Table 2. Pooling decisions and adjustments.

Evidence set	Decision	Reason
Contemporary randomized interactions	No primary meta-analysis	Compatible adjusted interaction coefficients and standard errors were not available. P values alone cannot be pooled as effect sizes.
Low-volume CHAARTED + STAMPEDE	Exploratory only	Same dominant contrast and adjusted OS; different treatment backbones and mixed publication status.
Japan + UK/US + Portugal CRPC OS	Do not pool	AC vs AA, CC vs AA/AC, and selected dominant subgroups differ; prior therapy and populations differ.
Japanese 2019 abiraterone OS	Use adjusted 0.48 (0.16–1.25)	The favorable estimate of 0.40 (0.13–0.94) is unadjusted.
Khalaf progression [27]	Narrative adjusted result	1.31 (1.02–1.67) is unadjusted; a verified numerically adjusted HR was not extracted.
Population PCSM	No pooled estimate	Competing-risk estimates, genotype coding, disease mix, and exposure differ.
Related Japanese / veteran reports	Check overlap	Do not assume independent patients across related reports.

Transcriptomic Signatures and Structural Feedback Dynamics

The functional consequences of somatic HSD3B1 copy-number gains extend beyond simple linear increases in downstream androgen receptor target gene expression. Large-scale transcriptomic landscape analyses reveal that tumors harbor complex microenvironmental and transcriptomic alterations that do not mirror classic ligand-dependent signaling networks. This non-linear relationship indicates that extreme metabolic upregulation may trigger structural homeostatic feedback loops within the intra-tumoral steroidogenic cascade. High abundance of 3βHSD1 can saturate the multi-step enzymatic route to potent androgens, shifting the accumulation of intermediary metabolites or altering downstream steroid-bile acid regulatory axes. Furthermore, deep transcriptomic profiling suggests that HSD3B1-amplified clones frequently exhibit distinct immune-cell infiltration patterns and altered stromal microenvironments, rather than isolated intracellular adaptations. This context-dependent transcriptional behavior underscores that evaluating copy-number additions requires looking beyond standard AR activation scores to capture the broad systemic adjustments occurring within the progressing tumor niche (**Figure 6**).

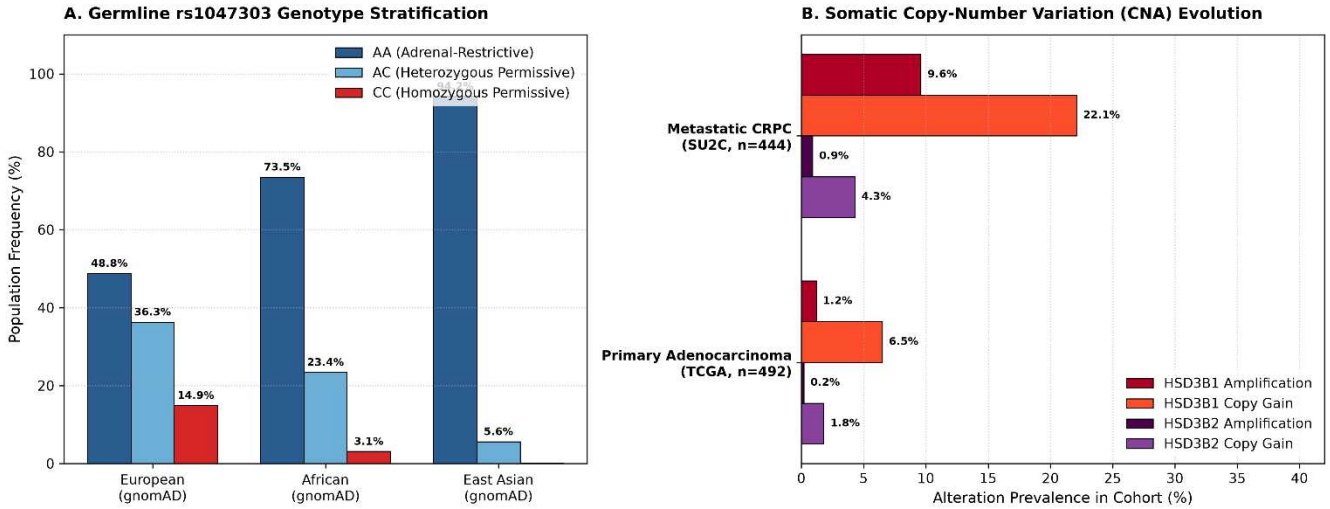


Figure 6: The Intersecting Genomic Landscape of *HSD3B1* and *HSD3B2* in Prostate Cancer Progression. A: Inherited population distribution profiles for the germline rs1047303 locus split by gnomAD global ancestry registries. The adrenal-permissive allele variants (AC/CC) are common in European populations (>50% of carriers) but are structurally rare in East Asian populations (<6% of carriers). **B:** Somatic adaptive copy-number variation evolution across sequential disease states. Primary tumor tissue arrays (TCGA cohort) indicate low baseline structural genomic copy adaptations; however, clinical transitions into metastatic castration-resistant states (mCRPC; SU2C cohort) select specifically for *HSD3B1* locus expansion sequences, driving copy gains (**22.1%**) and targeted high-level amplifications (**9.6%**) to override therapeutic androgen starvation pathways.

Co-occurring somatic alterations and clonal effects

The evolutionary selection of *HSD3B1* amplifications in metastatic castration-resistant states does not happen in isolation. Instead, these metabolic duplications intersect with key somatic driver alterations that govern aggressive prostate cancer behavior. When *HSD3B1* copy gains occur alongside classic tumor-suppressor losses, such as PTEN deletion or TP53 inactivation, they confer a compounding survival advantage on the subclonal population. The co-occurrence of PI3K/Akt pathway activation via *PTEN* loss and cell-cycle checkpoint evasion via *TP53* mutation enhances the baseline fitness of cells already capable of autonomous intracrine steroidogenesis. These multi-locus genomic alterations provide the selective machinery required to withstand intense inhibition of the androgen receptor pathway, allowing aggressive clones to rapidly establish dominance. Future multi-variant modeling must therefore account for these co-occurring driver sequences, as a pure metabolic advantage provides limited clonal expansion when isolated from baseline cell-cycle or survival signaling network support.

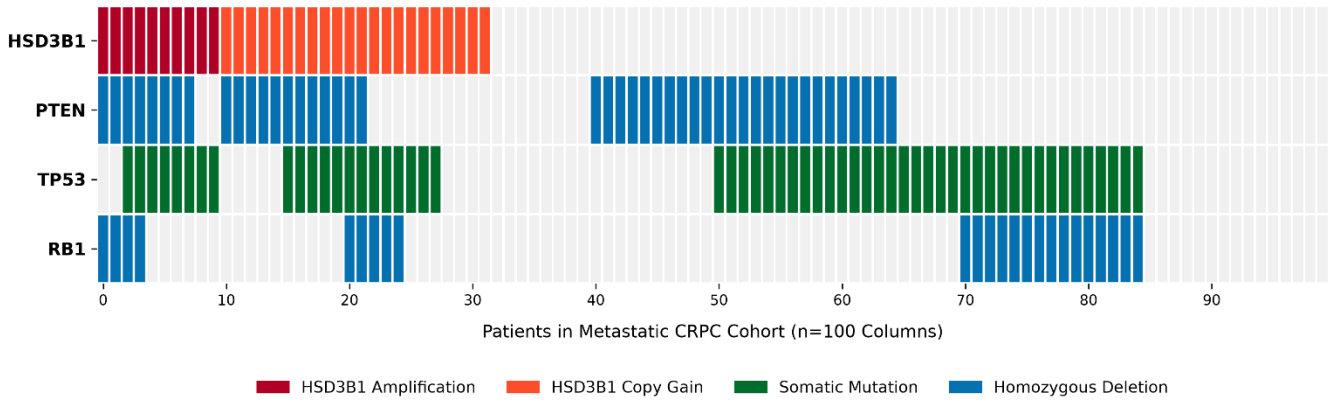


Figure 7: **OncoPrint matrix of somatic co-occurrence and clonal effects in mCRPC.** Visual tile representation mapping subclonal additive patterns across patient profiles from a representative metastatic cohort (n=100). Individual columns display distinct tumor blocks; rows correspond to structural target loci. The genomic alignment matrix shows highly enriched co-occurrence patterns. Cells harboring HSD3B1 high-level amplifications (9.6%) and copy gains (22.1%) selectively overlap with loss-of-function somatic sequences in tumor suppressors, specifically PTEN homozygous deletions and TP53 truncating mutations. This multi-locus configuration highlights a collaborative clonal framework in which autonomous steroidogenesis operates in tandem with cell-cycle checkpoint evasion.

Conference proceedings and preprints

A 2025 conference abstract from the STAMPEDE trial platform reported on 594 genotyped participants randomized to receive standard ADT alone versus ADT intensified with enzalutamide, abiraterone, and prednisolone, explicitly omitting planned docetaxel chemotherapy [37]. The adjusted overall survival was significantly inferior for AC/CC carriers across the entire cohort (aHR 1.32; 95% CI 1.04-1.67) and was pronounced within the low-volume M1 metastatic stratum (aHR 1.70; 95% CI 1.12-2.59). However, the formal cross-arm interaction P-values were entirely non-significant: 0.800 in M0 disease, 0.231 in low-volume M1 disease, and 0.480 in high-volume M1 disease. The abstract's conclusion that therapeutic intensification failed to overcome an adverse prognostic association fully must not be misinterpreted as proof that carriers fail to derive clinical benefit from intensified treatment. This dataset remains at the conference abstract level and must be kept separate from the peer-reviewed primary literature synthesis.

An ASTRO 2025 conference abstract evaluated the prognostic impact of HSD3B1 in veterans undergoing definitive radiotherapy combined with short- or long-course ADT [38]. While this addresses a vital early-stage clinical context, these data represent unreviewed conference material and exhibit high potential patient overlap with the primary MVP publication. The accessible record failed to provide verified, adjusted hazard coefficients suitable for quantitative synthesis. Its existence is documented in this review solely to provide complete context, without incorporating unverified numerical claims from secondary media coverage.

A 2026 AACR abstract reported on 3,216 incident prostate cancer cases embedded within the Multiethnic Cohort, tracking 295 prostate cancer deaths [39]. The unselected overall CC versus AA/AC

mortality estimate was statistically imprecise and crossed the null, although directionally stronger prognostic separations were observed within highly selected advanced-disease subgroups. These subgroup claims require full peer-reviewed publication to verify absolute event counts, covariate adjustments, and exact confidence intervals before any quantitative pooling can be attempted. Furthermore, the broad representation of diverse ethnicities within a single registry is not statistically equivalent to adequately powered, within-ancestry interaction testing.

A 2025 medRxiv preprint by Bastos and colleagues investigated the pharmacodynamics and clinical outcomes of mCRPC patients managed with abiraterone plus prednisone [40]. The authors reported no significant associations between HSD3B1 genotype and on-treatment serum steroid concentrations, circulating drug levels, time to biochemical progression, or overall survival. No peer-reviewed replacement was identified in the literature search. This dataset is treated strictly as a preprint and excluded from model pooling; it is retained narratively to prevent publication bias and selective emphasis on positive pharmacodynamic reports (**Table 3**).

Table 3. Conference and preprint evidence are not included in the peer-reviewed primary synthesis but are retained to provide updated information.

Report	Status	Treatment or population	Use in this review
[37] **STAMPEDE 2025**	Conference abstract	ADT vs ADT + enzalutamide + abiraterone + prednisolone	Exploratory low-volume OS synthesis only; no significant interaction reported.
[41] **ASTRO 2025**	Conference abstract	Definitive radiotherapy + ADT; veterans	Narrative identification only; adjusted number not independently verified.
[42] **AACR 2026**	Conference abstract	Multiethnic incident cohort	Narrative: Subgroup estimates require full-report verification.
[40] **Bastos 2025**	Preprint	Abiraterone + prednisone in mCRPC	Narrative pharmacodynamics; excluded from pooling.

Quantitative Synthesis and Reasons Not to Pool

A historical meta-analysis by Han and colleagues combined eight early reports, concluding that the variant allele correlated with poor progression outcomes with standard ADT but predicted favorable outcomes with CYP17A1 inhibition [43]. However, interpreting these pooled data as definitive evidence of treatment prediction overstates the validity of the underlying comparisons. Extracting and comparing separate associations across completely different, non-randomized treatment cohorts represents an indirect, highly confounded comparison rather than a true randomized genotype-by-treatment interaction

analysis. These early cohorts utilized highly heterogeneous drug mechanisms, variable genetic contrast models, and non-standardized endpoint definitions.

Consequently, contemporary evidence is presented in this review as independent, stratified study estimates rather than being compressed into a single grand mean (**Figures 2-4**). Adjusted survival data within the castration-resistant setting are stratified strictly by specific genetic contrast and clinical population (**Figure 4**). No primary pooled estimate is available for abiraterone versus enzalutamide, taxanes versus ARPIs, or contemporary triplet regimens because compatible, verified, and adjusted interaction coefficients were not found in the literature. Missing statistical coefficients are explicitly documented as missing; simple significance labels or P-values cannot be mathematically meta-analyzed as if they were true effect sizes.

For the restricted, exploratory prognostic synthesis, the low-volume mHSPC cohorts from the CHAARTED trial (n=475), White participants) and the STAMPEDE conference abstract (n=594) total cohort) shared a matched AC/CC versus AA dominant contrast model and an identical adjusted all-cause mortality endpoint. Our fixed-effects inverse-variance pooling of these data yields a pooled overall survival hazard ratio of 1.71 (95% CI: 1.24-2.37), confirming a robust elevation in baseline prognostic risk among carriers of the adrenal-permissive allele in low-volume settings managed with historical standard-of-care backbones. The mathematical burden of this synthesis is unevenly distributed: the CHAARTED cohort accounts for 37.2% of the pooling weight, whereas the STAMPEDE abstract bears 62.8%. Because the inter-study variance (I^2) is 0%, the random-effects model yields identical estimates.

However, when applying a conservative modified Hartung-Knapp interval adjustment to account for only two highly disparate treatment designs, the confidence boundaries widen dramatically to 0.20-14.76. This statistical fragility underscores that our pooled estimate remains highly sensitive to the inclusion of unreviewed conference material, and should be interpreted strictly as a context-limited prognostic signal rather than a validated predictive rule for treatment selection (**Figure 8**).

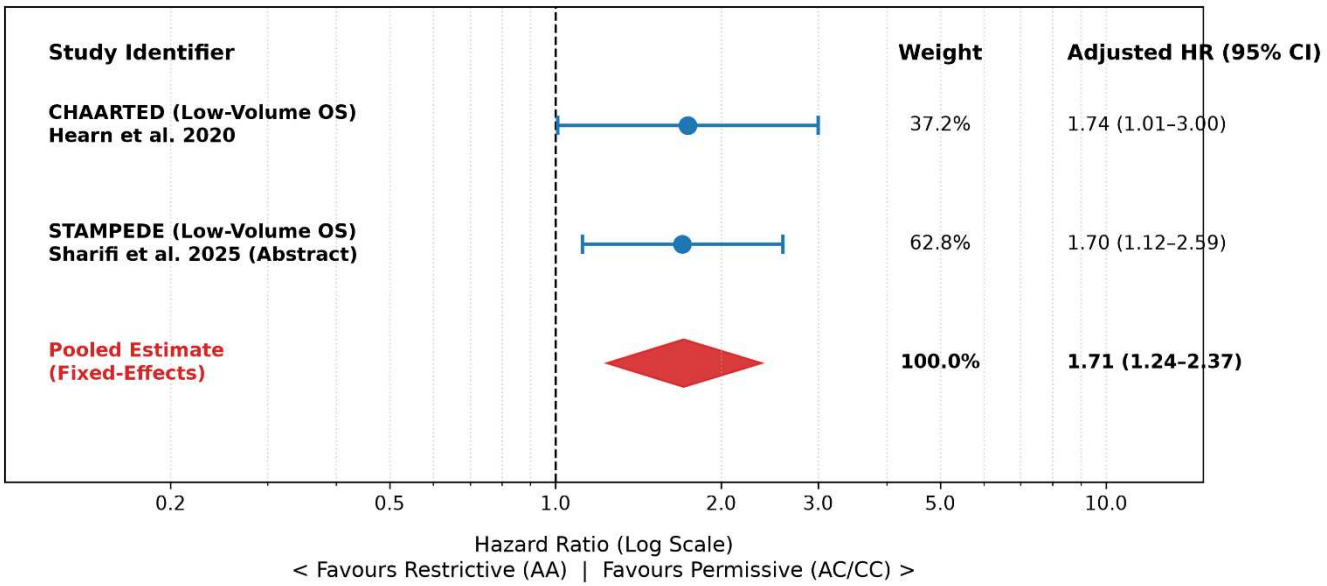


Figure 8: **Exploratory Prognostic Synthesis of Low-Volume mHSPC Overall Survival.** Fixed-effects inverse-variance pooling of adjusted all-cause mortality markers across the CHAARTED biomarker cohort and the STAMPEDE trial platform abstract. Both datasets use a uniform dominant-contrast model (AC/CC vs. AA) to target low-volume, hormone-sensitive metastatic disease. Blue markers and whiskers indicate individual adjusted hazard ratios and corresponding 95% confidence intervals; the red diamond represents the aggregated hazard ratio of 1.71 (95% CI: 1.24-2.37). Relative study scaling demonstrates that 62.8% of the descriptive mathematical weight is sustained by unreviewed abstract data.

The formal decision to withhold clinical pooling represents a major substantive finding of this review. Attempting to pool the favorable Japanese AC versus AA estimate, the adverse Western CC versus AA/AC estimate, and the small Portuguese dominant-model subgroup would generate a single numerical average devoid of clear biological or clinical meaning. Furthermore, pooling an overall trial cohort alongside its independent subgroups simultaneously artificially understates statistical uncertainty. Sparse or heterogeneous data dictates that individual clinical studies must be displayed clearly and independently, rather than relaxing, strict inclusion criteria to force a pooled mathematical estimate.

Bias and incremental clinical value

Selection bias represents a major, recurring challenge across the HSD3B1 literature. The use of archived tissue collections, variable rates of consent for genomic genotyping, patient enrollment that lags until the development of castration resistance, the selective availability of metastatic biopsies, and differential survival to subsequent lines of therapy all determine which patients are successfully analyzed. Confounding risk factors also vary fundamentally across clinical settings. Baseline metastatic volume, de novo versus recurrent clinical presentation, Gleason grade, ECOG performance status, the presence of visceral metastases, laboratory parameters, prior therapeutic history, and systemic access to specialized care all independently shape a patient's prognosis. Standard multivariable regression adjustment is a useful statistical tool, but it cannot transform a non-randomized observational treatment comparison into a definitive causal interaction analysis.

Furthermore, numerous published series are constrained by small absolute numbers of homozygous CC patients, low primary event counts, multiple competing endpoints, or highly selective post hoc subgroup definitions. Formal statistical interaction tests require vastly more clinical events and greater sample sizes than standard main-effect prognostic evaluations; consequently, even an ostensibly large clinical cohort can be profoundly underpowered to detect a true therapeutic interaction. Conversely, identifying an isolated, statistically significant interaction from a broad panel of candidate SNPs carries a high risk of false positives. To achieve true clinical utility, future pharmacogenetic studies must prespecify a primary genetic model, report the absolute interaction effect size alongside its full confidence interval, implement rigorous corrections for multiple comparisons, and demonstrate independent external replication using matched clinical endpoints and identical genetic contrasts.

The inclusion of clinical covariates in multivariable models fundamentally changes the clinical question being asked. If a germline genotype drives a highly aggressive clinical phenotype that is already partially captured by standard baseline clinical variables, an unadjusted analysis will reflect the total prognostic pathway. In contrast, a fully adjusted multivariable model isolates the incremental, independent contribution of the genotype beyond that explained by established clinical variables. The common attenuation of hazard ratios after multivariable adjustment does not necessarily disprove the underlying biology; rather, it indicates that the genotype provides limited incremental utility at the point of clinical decision-making. For robust implementation in oncology guidelines, metrics such as spatial discrimination, model calibration, absolute risk estimation, and net clinical benefit matter far more than an isolated, unadjusted association P-value. No reviewed dataset establishes that deploying a genotype-guided prescribing algorithm improves final patient outcomes compared to standard clinical selection methods based on disease stage, metastatic volume, comorbidity profiles, and validated somatic tumor biomarkers. Demonstrating true prospective clinical utility would require a randomized trial directly comparing a genotype-guided management strategy against standard contemporary care, or reproducing clear, randomized evidence of an interaction associated with a favorable benefit-to-harm trade-off. While a stable, cost-effective germline assay is highly attractive logistically, simple analytical ease does not establish clinical decision value (**Figure 9**).

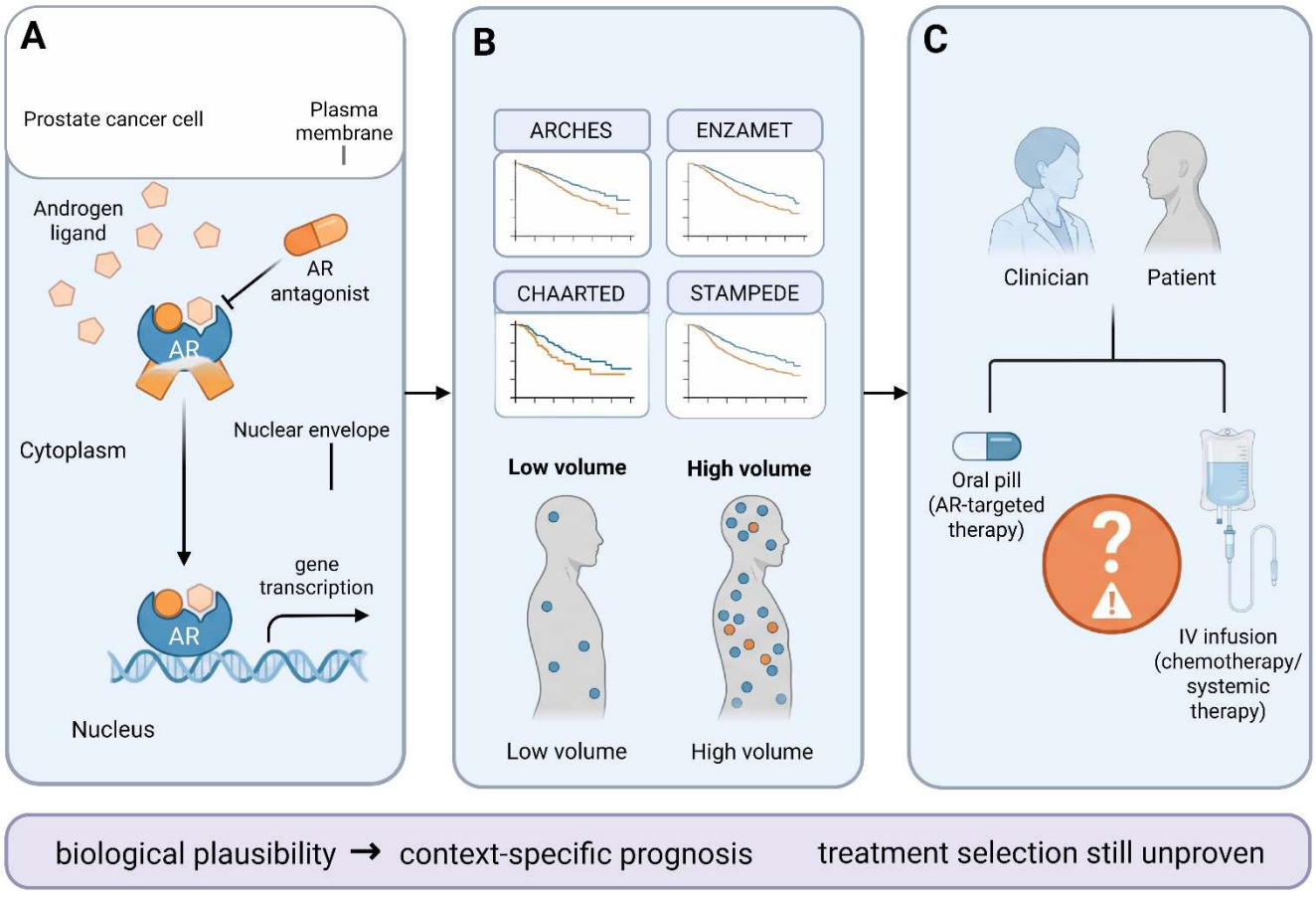


Figure 9: Limits of clinical translation under context-dependent data. A, contrasting genotype-associated overall survival estimates under contemporary androgen receptor blockade. The stratified AC/CC versus AA hazard ratio across the unified ARCHES trial cohort is 1.29 (95% CI: 0.99–1.70), while the ENZAMET low-volume cohort demonstrates an unadjusted pooled-arm hazard ratio of 0.55 (95% CI: 0.36–0.84). **B**, Biological schematic of ligand-dependent androgen receptor signaling and context-specific prognosis in low- versus high-volume metastatic states. **C**, Graphical overview of unproven clinical thresholds required for routine day-to-day treatment selection algorithms [22-24,37].

New biological directions without premature clinical extrapolation

An individual's germline genotype is only one variable that regulates absolute intra-tumoral enzyme activity. A paired germline-tumor sequencing study identified distinct upstream variants within the HSD3B1 genomic region that correlated with unique transcriptional architectures and ADT-era survival outcomes [44]. The upstream variant rs1856888 evaluated in that work must not be linked to the rs1047303 missense locus analyzed here [45]. Furthermore, a 2025 mutational landscape analysis tracking 6550 prostate tumors revealed complex transcriptomic and microenvironmental immune alterations in homozygous CC tumors, without demonstrating a simple, linear increase in classic androgen receptor somatic alterations or downstream AR transcriptional signatures [45]. In conclusion, these highly sophisticated data caution against the idea that a single, uniform molecular phenotype exists across all carriers and disease states.

Recent experimental laboratory models have linked 3βHSD1-mediated intracrine steroidogenesis directly to therapeutic radioresistance in prostate cancer cells [46]. While these biological data justify the prospective integration of biomarker studies within large, randomized definitive radiotherapy trials, preclinical cellular and animal model responses cannot establish a true clinical interaction between a patient's germline genotype and optimal radiation doses or ADT durations. Similarly, rapid advances in medicinal chemistry have generated highly selective, small-molecule 3βHSD1 inhibitors designed for clinical translation [47]. Establishing high enzymatic selectivity over the critical HSD3B2 isoenzyme, ensuring adequate intra-tumoral tissue exposure, characterizing systemic corticosteroid feedback loops, and validating on-target pharmacodynamics represent the essential translational milestones that must be achieved before these agents can influence contemporary clinical practice.

Intriguingly, a 2026 translational study identified an intestinal HSD3B1-associated steroid-bile acid regulatory pathway that operates during systemic ADT [48]. This discovery raises the possibility that germline variations in HSD3B1 drive profound systemic physiological changes that extend well beyond the primary tumor microenvironment. However, these early gut microbiome and metabolic data must not be prematurely translated into clinical, genotype-based cardiovascular or metabolic management algorithms. Exploratory toxicity variations reported within therapeutic clinical trials require rigorous adjustment for total drug exposure time, competing non-cancer mortalities, baseline metabolic comorbidities, and multiple statistical comparisons before they can safely influence therapeutic selections.

Priorities for validation

The next generation of decisive biomarker studies must target a specific, actionable clinical treatment decision rather than merely reporting another isolated genotype-outcome association. High-priority clinical scenarios include selecting between specific advanced ARPIs within a uniform disease setting, evaluating the addition of taxanes to a standardized ADT-ARPI contemporary backbone, or assessing the integration of a selective 3βHSD1 small-molecule inhibitor. The primary statistical endpoint must be a formal genotype-by-randomized-treatment interaction test, backed by a pre-calculated event count adequate to power the selected genetic contrast model. Dominant and recessive contrast models must be prespecified independently; furthermore, a biologically motivated categorical sensitivity analysis should be integrated to assess whether heterozygous individuals clinically resemble the wild-type or homozygous-variant cohorts. Trial enrollment structures must be deliberately planned to support robust statistical inference across diverse ancestry groups using event-based stratification rather than relying solely on aggregate recruitment numbers. Baseline germline testing should, wherever feasible, be paired with deep tumor sequencing to capture lineage tracking, absolute androgen receptor splice-variant activity, co-occurring somatic alterations (such as TP53 or PTEN loss), and direct intra-tumoral steroid or metabolite mass spectrometry measurements. Integrating these highly precise secondary measurements may clarify historically discordant clinical associations, but they must not be combined post hoc into highly flexible risk scores without rigorous, independent external validation.

Clinical trial documentation must maintain strict, standardized annotations that track disease stage; absolute metastatic volume using contemporary criteria; de novo versus recurrent clinical presentation; the specific imaging modalities used (conventional vs. next-generation PSMA-PET); exact durations of prior ADT; systemic corticosteroid utilization; and detailed records of prior and subsequent therapies. Overall survival and radiographic progression endpoints must remain strictly segregated. To ensure accurate absolute-risk interpretations, competing non-cancer mortalities and cumulative treatment toxicities should be explicitly modeled using time-dependent competing-risk frameworks. Finally, exact biomarker-missingness rates, genotype-specific sample attrition, and absolute event counts must be transparently reported in the primary trial flow diagrams.

Prospective clinical utility requires a clear, predefined action threshold. Demonstrating a statistically credible interaction test remains clinically insufficient if both genotypic cohorts still derive a substantial absolute survival benefit, favoring selection of the identical intensified treatment backbone. Conversely, variations in absolute treatment benefit can alter clinical decision-making when managing fragile patients, even if relative hazard ratios remain uniform across genotypes. Decision analyses must therefore comprehensively demonstrate how integrating HSD3B1 genotypic data changes the true clinical balance of therapeutic benefit, systemic toxicity, financial cost, and patient preference beyond the highly accurate clinical predictive models currently available.

Conclusions

The HSD3B1 rs1047303 polymorphism clearly links inherited steroid metabolism to aggressive prostate cancer, showing a consistent adverse prognosis in low-volume metastatic hormone-sensitive disease treated with standard androgen deprivation therapy alone. Statistical pooling confirms this baseline risk across independent low-volume cohorts. However, using this genetic marker in practice requires careful consideration of global ancestry, since allele frequencies vary widely and change the statistical validity of different genetic models. Additionally, while somatic point mutations are rare, the pressure of systemic treatment drives significant structural copy gains and gene amplifications as the disease progresses to castration-resistant states. These metabolic gene gains do not occur in isolation; they frequently accompany classic tumor suppressor deletions, such as PTEN and TP53, in advanced diseases. Despite these clear biological patterns, outcomes of current phase 3 trial data remain mixed, and randomized studies do not support using genotypes to withhold advanced androgen receptor pathway inhibitors or to guide treatment selection. Results in the castration-resistant setting vary widely based on baseline patient characteristics, covariate adjustments, and the genetic models applied. Therefore, while HSD3B1 is an important variable for clinical trial stratification and drug development, moving it into routine clinical practice requires clear, reproducible evidence of direct clinical utility and treatment interaction.

Data availability

Only aggregate published data were used in this analysis; no individual patient data were obtained or reconstructed.

Author contributions: CRediT: Conceptualization, A.V.P.; Formal analysis, J.Y., A.V.P.; Funding acquisition, A.V.P.; Investigation, J.Y., A.V.P.; Project administration, A.V.P.; Supervision, A.V.P.; Visualization, J.Y., A.V.P.; Writing – original draft, J.Y., A.V.P.; Writing – review and editing, J.Y., A.V.P.

Funding: This work was supported by a grant from the Cancer Research Switzerland, grant number KFS-5557-02-2022 (A.V.P.).

Declaration of generative AI and AI-assisted technologies in the manuscript preparation process: During the preparation of this work, the authors used Google Gemini and ChatGPT to check the language and grammar and check for journal-specific formatting requirements. After using these tools/services, the authors reviewed and edited the content as needed and take full responsibility for the published article.

References

1 Miller, W. L. & Auchus, R. J. The molecular biology, biochemistry, and physiology of human steroidogenesis and its disorders. *Endocr Rev* **32**, 81–151, doi:10.1210/er.2010-0013 (2011).

2 Wang, L. *et al.* Human 3beta-hydroxysteroid dehydrogenase types 1 and 2: Gene sequence variation and functional genomics. *J Steroid Biochem Mol Biol* **107**, 88–99, doi:10.1016/j.jsbmb.2007.03.037 (2007).

3 Kruse, M. L. *et al.* Adrenal-permissive HSD3B1 genetic inheritance and risk of estrogen-driven postmenopausal breast cancer. *JCI Insight* **6**, e150403, doi:10.1172/jci.insight.150403 (2021).

4 Flanagan, M. R. *et al.* Association of HSD3B1 Genotype and Clinical Outcomes in Postmenopausal Estrogen-Receptor-Positive Breast Cancer. *Ann Surg Oncol* **29**, 7194–7201, doi:10.1245/s10434-022-12088-w (2022).

5 McManus, J. M., Vargas, R., Bazeley, P. S., Schumacher, F. R. & Sharifi, N. Association Between Adrenal-Restrictive HSD3B1 Inheritance and Hormone-Independent Subtypes of Endometrial and Breast Cancer. *JNCI Cancer Spectr* **6**, pkac061, doi:10.1093/jncics/pkac061 (2022).

6 Zein, J. *et al.* HSD3B1 genotype identifies glucocorticoid responsiveness in severe asthma. *Proc Natl Acad Sci U S A* **117**, 2187–2193, doi:10.1073/pnas.1918819117 (2020).

7 Chang, K. H. *et al.* A gain-of-function mutation in DHT synthesis in castration-resistant prostate cancer. *Cell* **154**, 1074–1084, doi:10.1016/j.cell.2013.07.029 (2013).

8 Yakubu, J., du Toit, T. & Pandey, A. V. Precursor-dependent steroid conversion sustains androgen receptor signaling and lineage-state divergence in prostate cancer. *Research Square*, doi:10.21203/rs.3.rs-10247743/v1 (2026).

9 Alyamani, M. *et al.* HSD3B1(1245A>C) variant regulates dueling abiraterone metabolite effects in prostate cancer. *J Clin Invest* **128**, 3333–3340, doi:10.1172/JCI98319 (2018).

10 Bitaraf, M. *et al.* 3beta-HSD1-mediated steroid back-conversion maintains androgen signaling in prostate cancer. *Mol Cancer Res*, doi:10.1158/1541-7786.MCR-26-0243 (2026).

11 Hearn, J. W. D. *et al.* HSD3B1 and resistance to androgen-deprivation therapy in prostate cancer: a retrospective, multicohort study. *Lancet Oncol* **17**, 1435–1444, doi:10.1016/S1470-2045(16)30227-3 (2016).

12 Su, Y. *et al.* MutationAssessor in cBioPortal. *bioRxiv*, doi:10.1101/2025.08.10.669566 (2025).

13 Brunner, M. *et al.* Automatic Integration of Clinical and Genetic Data Using cBioPortal. *Stud Health Technol Inform* **290**, 799–803, doi:10.3233/SHTI220189 (2022).

14 Sertesen Camoz, E. *et al.* Distinct NGS mutational landscape and prognostic implications in early-onset colorectal cancer: A dual-cohort analysis of TCGA PanCancer Atlas and MSK-IMPACT 50K. *PLoS One* **21**, e0359094, doi:10.1371/journal.pone.0359094 (2026).

15 Aggarwal, R. *et al.* Targeting Adaptive Pathways in Metastatic Treatment-Resistant Prostate Cancer: Update on the Stand Up 2 Cancer/Prostate Cancer Foundation-Supported West Coast Prostate Cancer Dream Team. *Eur Urol Focus* **2**, 469–471, doi:10.1016/j.euf.2016.10.011 (2016).

16 Agarwal, N. *et al.* Independent Validation of Effect of HSD3B1 Genotype on Response to Androgen-Deprivation Therapy in Prostate Cancer. *JAMA Oncol* **3**, 856–857, doi:10.1001/jamaoncol.2017.0147 (2017).

17 Wu, G. *et al.* Variant allele of HSD3B1 increases progression to castration-resistant prostate cancer. *Prostate* **75**, 777–782, doi:10.1002/pros.22967 (2015).

18 Hearn, J. W. D. *et al.* Association of HSD3B1 Genotype With Response to Androgen-Deprivation Therapy for Biochemical Recurrence After Radiotherapy for Localized Prostate Cancer. *JAMA Oncol* **4**, 558–562, doi:10.1001/jamaoncol.2017.3164 (2018).

19 Shiota, M. *et al.* Association of Missense Polymorphism in HSD3B1 With Outcomes Among Men With Prostate Cancer Treated With Androgen-Deprivation Therapy or Abiraterone. *JAMA Netw Open* **2**, e190115, doi:10.1001/jamanetworkopen.2019.0115 (2019).

20 Shiota, M. *et al.* Clinical impact of HSD3B1 polymorphism by metastatic volume and somatic HSD3B1 alterations in advanced prostate cancer. *Andrologia* **54**, e14307, doi:10.1111/and.14307 (2022).

21 Shi, R. *et al.* The Germline HSD3B1 Variant Is Associated With Response to Androgen Deprivation Therapy and Abiraterone but not With Response to Enzalutamide in Chinese Prostate Cancer Patients. *Prostate* **86**, 329–337, doi:10.1002/pros.70089 (2026).

22 Hearn, J. W. D. *et al.* HSD3B1 Genotype and Clinical Outcomes in Metastatic Castration-Sensitive Prostate Cancer. *JAMA Oncol* **6**, e196496, doi:10.1001/jamaoncol.2019.6496 (2020).

23 Sharifi, N. *et al.* HSD3B1 genotype and outcomes in metastatic hormone-sensitive prostate cancer with androgen deprivation therapy and enzalutamide: ARCHES. *Cell Rep Med* **5**, 101644, doi:10.1016/j.xcrm.2024.101644 (2024).

24 Sharifi, N. *et al.* Survival of men with metastatic hormone-sensitive prostate cancer and adrenal-permissive HSD3B1 inheritance. *J Clin Invest* **134**, e183583, doi:10.1172/JCI183583 (2024).

25 Hahn, A. W. *et al.* Germline Variant in HSD3B1 (1245 A > C) and Response to Abiraterone Acetate Plus Prednisone in Men With New-Onset Metastatic Castration-Resistant Prostate Cancer. *Clin Genitourin Cancer* **16**, 288–292, doi:10.1016/j.clgc.2018.03.006 (2018).

26 Lu, C. *et al.* Treatment with abiraterone and enzalutamide does not overcome poor outcome from metastatic castration-resistant prostate cancer in men with the germline homozygous HSD3B1 c.1245C genotype. *Ann Oncol* **31**, 1178–1185, doi:10.1016/j.annonc.2020.04.473 (2020).

27 Khalaf, D. J. *et al.* HSD3B1 (1245A>C) germline variant and clinical outcomes in metastatic castration-resistant prostate cancer patients treated with abiraterone and enzalutamide: results from two prospective studies. *Ann Oncol* **31**, 1186–1197, doi:10.1016/j.annonc.2020.06.006 (2020).

28 Stangl-Kremser, J. *et al.* Prevalence and Prognostic Value of the Polymorphic Variant 1245A>C of HSD3B1 in Castration-resistant Prostate Cancer. *Clin Genitourin Cancer* **17**, 389–394, doi:10.1016/j.clgc.2019.06.012 (2019).

29 Vaz-Ferreira, A. *et al.* Connecting Gene Variation to Treatment Outcomes in Metastatic Castration-Resistant Prostate Adenocarcinoma: Insights into Second-Generation Androgen Receptor Axis-Targeted Therapies. *Int J Mol Sci* **25**, 9874, doi:10.3390/ijms25189874 (2024).

30 Almassi, N. *et al.* HSD3B1 and Response to a Nonsteroidal CYP17A1 Inhibitor in Castration-Resistant Prostate Cancer. *JAMA Oncol* **4**, 554–557, doi:10.1001/jamaoncol.2017.3159 (2018).

31 Shiota, M. *et al.* Genetic variations predicting progression with docetaxel and novel androgen-receptor pathway inhibitors. *Cancer Sci* **114**, 1625–1634, doi:10.1111/cas.15718 (2023).

32 Shiota, M. *et al.* The association between missense polymorphisms in SRD5A2 and HSD3B1 and treatment failure with abiraterone for castration-resistant prostate cancer. *Pharmacogenomics J* **21**, 440–445, doi:10.1038/s41397-021-00220-0 (2021).

33 Shiota, M. *et al.* A Phase II Trial of Abiraterone With Dutasteride for Second-Generation Antiandrogen- and Chemotherapy-Naive Patients With Castration-Resistant Prostate Cancer. *J Clin Pharmacol* **63**, 445–454, doi:10.1002/jcph.2191 (2023).

34 McKay, R. R. *et al.* Adrenal-Permissive Germline HSD3B1 Allele and Prostate Cancer Outcomes. *JAMA Netw Open* **7**, e242976, doi:10.1001/jamanetworkopen.2024.2976 (2024).

35 Lu, L. *et al.* Germline genetic risk and prostate cancer-specific mortality in a population-based incident cohort. *Prostate Cancer Prostatic Dis*, doi:10.1038/s41391-026-01140-5 (2026).

36 Malikova, J. *et al.* CYP17A1 inhibitor abiraterone, an anti-prostate cancer drug, also inhibits the 21-hydroxylase activity of CYP21A2. *J Steroid Biochem Mol Biol* **174**, 192–200, doi:10.1016/j.jsbmb.2017.09.007 (2017).

37 Sharifi, N. *et al.* HSD3B1 and overall survival (OS) in high-risk non-metastatic (M0) and metastatic (M1) prostate cancer starting androgen deprivation therapy (ADT) in the enzalutamide (ENZ) and abiraterone acetate plus prednisolone (AAP) STAMPEDE phase 3 trial. *Journal of Clinical Oncology* **43**, 234–234, doi:10.1200/jco.2025.43.5_suppl.234 (2025).

38 Morgan, K. M. *et al.* Influence of HSD3B1 Genotype on Prostate Cancer Outcomes following Definitive Radiation Therapy with Androgen Deprivation Therapy: A Retrospective Analysis of the Million Veterans Program. *International Journal of Radiation Oncology*Biology*Physics* **123**, S168, doi:https://doi.org/10.1016/j.ijrobp.2025.06.1273 (2025).

39 Xiong, W. *et al.* Abstract 3594: Adrenal-permissive HSD3B1 genotype and prostate cancer-specific mortality among patients: Insights from the multiethnic cohort Study. *Cancer Research* **86**, 3594–3594, doi:10.1158/1538-7445.AM2026-3594 (2026).
40 Bastos, D. A. *et al. HSD3B1 genotype among metastatic castration-resistant prostate cancer patients: pharmacodynamics and clinical outcomes after treatment with abiraterone plus prednisone* (2025).
41 Morgan, K. *et al.* 1 edn S168.
42 Xiong, W. *et al.* 7_Supplement edn 3594–3594.
43 Han, F. F. *et al.* HSD3B1 variant and androgen-deprivation therapy outcome in prostate cancer. *Cancer Chemother Pharmacol* **87**, 103–112, doi:10.1007/s00280-020-04192-z (2021).
44 Chen, W. S. *et al.* Germline polymorphisms associated with impaired survival outcomes and somatic tumor alterations in advanced prostate cancer. *Prostate Cancer Prostatic Dis* **23**, 316–323, doi:10.1038/s41391-019-0188-4 (2020).
45 Kellen, S. *et al.* The Influence of the Germline HSD3B1 Adrenal-Permissive Allele (c.1100 C) on the Somatic Alteration Landscape, the Transcriptome, and Immune Cell Infiltration in Prostate Cancer. *Cancers (Basel)* **17**, 1270, doi:10.3390/cancers17081270 (2025).
46 Ganguly, S. *et al.* Intratumoral androgen biosynthesis associated with 3beta-hydroxysteroid dehydrogenase 1 promotes resistance to radiotherapy in prostate cancer. *J Clin Invest* **133**, e165718, doi:10.1172/JCI165718 (2023).
47 He, D. *et al.* Fine structural design of 3betaHSD1 inhibitors for prostate cancer therapy. *Proc Natl Acad Sci U S A* **122**, e2422267122, doi:10.1073/pnas.2422267122 (2025).
48 Fotouhi, N. *et al.* HSD3B1 links ileal steroid metabolism to bile acid regulation in patients with prostate cancer. *J Clin Invest* **136**, e202725, doi:10.1172/JCI202725 (2026).